Stepwise Modification of a Modular Enhancer Underlies Adaptation in a *Drosophila* Population

Mark Rebeiz,[1] John E. Pool,[2,3] Victoria A. Kassner,[1] Charles F. Aquadro,[4] Sean B. Carroll[1]*

The evolution of cis regulatory elements (enhancers) of developmentally regulated genes plays a large role in the evolution of animal morphology. However, the mutational path of enhancer evolution—the number, origin, effect, and order of mutations that alter enhancer function—has not been elucidated. Here, we localized a suite of substitutions in a modular enhancer of the *ebony* locus responsible for adaptive melanism in a Ugandan *Drosophila* population. We show that at least five mutations with varied effects arose recently from a combination of standing variation and new mutations and combined to create an allele of large phenotypic effect. We underscore how enhancers are distinct macromolecular entities, subject to fundamentally different, and generally more relaxed, functional constraints relative to protein sequences.

Three major challenges for understanding the genetic and molecular bases of morphological evolution are to identify loci underlying trait divergence, to pinpoint functional changes within these loci, and to trace the origin of functional variation in populations. The evolution of animal morphological diversity is generally associated with changes in the spatial expression of genes that govern development (*1*, *2*). The divergence of particular morphological traits has been linked to changes in specific enhancers of individual loci (*3*–*9*). Mutations in individual, modular enhancers are thought to circumvent the potentially pleiotropic effects of mutations in coding sequences of genes that participate in many developmental processes (*10*–*12*).

Nonetheless, there is relatively little detailed knowledge of how enhancer sequences evolve, of the genetic path of enhancer evolution. In most instances, functional mutations have not been identified, so their individual effects and origins have not been traced. In contrast, the evolutionary paths of several proteins have been traced and revealed that many trajectories, including reversals, are not allowed because of structural constraints (*13*–*15*). To decipher the mode and tempo of regulatory sequence evolution, we must determine the following: How many mutations are involved in enhancer divergence? What effects do individual mutations have? And, what is the relative contribution of standing variation and new mutations to enhancer evolution?

To identify enhancers that have recently evolved, we have traced the recent evolution of adaptive pigmentation within African populations of *Drosophila melanogaster*. We elucidate a specific set of regulatory mutations that underlie changes in gene expression and pigmentation and reconstruct the path of enhancer evolution.

Adaptive melanism in a *Drosophila* population. Across Africa, a strong correlation exists between elevation and the degree of abdominal pigmentation in *D. melanogaster* populations (*16*). This correlation is not explained by population structure, indicating that dark pigmentation is a derived adaptation to high altitude or a correlating selective pressure. Previous study of a dark population from Uganda (*16*) uncovered a partial selective sweep at the *ebony* locus, where the darkest third chromosome lines (Fig. 1) share a 14-kilobase haplotype block of nearly identical sequence extending over the noncoding region of the *ebony* locus (fig. S1). *ebony* encodes a pleiotropic, multifunctional enzyme in the biogenic amine synthesis pathway (*17*) that functions in a variety of processes. In the adult cuticle, expression of *ebony* is required in regions that will generate a yellow shade (*18*), and its absence causes a dark, melanic cuticular phenotype.

The partial sweep at the *ebony* locus and its association with dark pigmentation is evidence that genetic variation at *ebony* contributes to the melanic phenotype (*16*). To test this association directly, we undertook a series of transgenic complementation experiments with use of *ebony* transgenes from light (U62) and dark (U76) extraction lines. In an *ebony* null mutant background, we found that the pigmentation phenotypes of animals bearing the light (U62) and dark (U76) transgenes differed by about 10 pigmentation units (figs. S2A and S3). This is similar to the magnitude of pigmentation difference between the U76 and U62 extraction lines (fig. S2A). Furthermore, in the genetic background of the dark U76 line, we found that a single copy of the light (U62) transgene was sufficient to fully complement the melanic abdominal phenotype (fig. S2B). These results suggest that variation at *ebony* can account for much of the phenotypic variation between extraction lines.

In addition, on the basis of the identification below of haplotypes containing causative mutations, we used a standard analysis of variance approach to estimate the contribution of these haplotypes to phenotypic differences. We found that variation at *ebony* accounts for up to 83% of the total phenotypic variation [supporting online material (SOM) text]. These results confirm that *ebony* is the major locus responsible for the dark phenotype of the Ugandan extraction lines.

Noncoding variation at *ebony* causes abdominal melanism. The association between variation at *ebony* and melanic pigmentation could be due to divergence in the regulation of *ebony* expression and/or protein function. However, among the light and dark transgenes tested, the dark allele contained no derived coding differences relative to the species consensus (fig. S4), and only one derived difference existed in the light U62 line (P46T), suggesting that causative changes lie outside the coding region. To test whether a transcriptional regulatory difference may be responsible for the dark pheno-

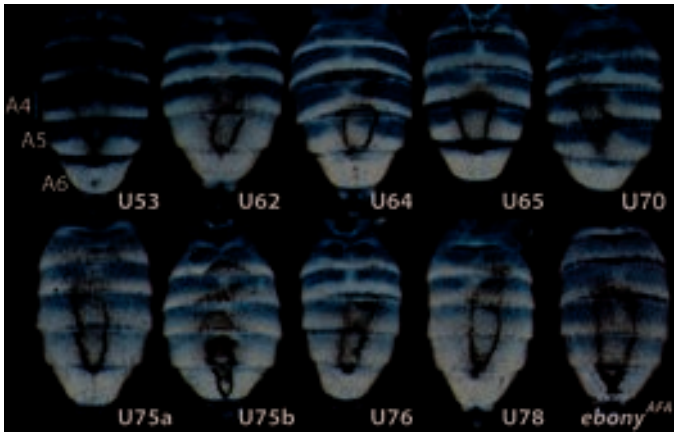

Fig. 1. Variation in abdominal pigmentation within a Ugandan population of *D. melanogaster*. Each abdomen is derived from an extraction line bearing a homozygous third chromosome from a Ugandan population sample. The name of each line designates the percent darkness of the A4 abdominal tergite. *ebony*^{AFA} is a null mutation.

[1]Howard Hughes Medical Institute and Laboratory of Molecular Biology, University of Wisconsin, Madison, WI 53706, USA. [2]Department of Integrative Biology, University of California, Berkeley, CA 94720, USA. [3]Center for Population Biology, University of California, Davis, CA 95616, USA. [4]Department of Molecular Biology and Genetics, Cornell University, Ithaca, NY 14850, USA.

*To whom correspondence should be addressed. E-mail: sbcarrol@wisc.edu

type, *ebony* mRNA expression in newly eclosed adults was visualized by in situ hybridization (Fig. 2). There was a marked reduction (58 to 83%) in *ebony* mRNA expression in darker lines (Fig. 2 and table S1). The association of the dark phenotype and haplotype with decreased *ebony* mRNA suggests that cis regulatory sequence mutations have accumulated that reduce *ebony* expression.

To localize regions of the *ebony* locus responsible for the dark phenotype, we tested the activity of chimeric *ebony* transgenes in which the upstream regulatory region of each allele was fused to the downstream first exon and coding region of the other allele. The light/dark construct performed nearly as well as the light construct in complementing the abdominal phenotype of an *ebony* null mutant (Fig. 3, C and G), whereas the reciprocal dark/light transgene yielded a phenotype similar to that of the complete dark allele construct (Fig. 3, D and G). The phenotypes of the chimeric transgenes indicate that the functional differences between the light and dark alleles largely reside in the 5′ noncoding region of the locus, presumably within enhancers.

Regulatory divergence at ebony is restricted to a modular enhancer. To identify enhancers within the *ebony* regulatory region (figs. S5 and S6), we fused fragments of noncoding DNA to a green fluorescent protein (GFP) reporter gene and monitored reporter expression in adult tissues. We identified an array of modular enhancers with activities in many tissues that exhibit *ebony* mutant phenotypes or that express the gene (Fig. 4A and fig. S5). One enhancer active in the developing abdomen (and thorax) was localized to a 0.7-kb fragment located 3.6 kb upstream of the *ebony* promoter ("abd" in Fig. 4A). The abdominal element drove reporter expression in a broader domain than that of the native *ebony* expression pattern, including the posterior regions of each tergite (fig. S6H) and the male A5 and A6 segments (fig. S6, E and F). However, the extension of reporter constructs to include promoter-proximal and intronic sequences resulted in a precise recapitulation of the endogenous *ebony* expression pattern (fig. S6, N and T).

Regulatory mutations are suggested to minimize pleiotropic effects relative to coding mutations because of the modular organization of cis regulatory regions (*10*–*12*). However, the modularity of enhancers has not yet been tested with naturally occurring mutations in a comprehensively defined regulatory region. To examine whether regulatory mutations in one module impact the function of adjacent modules, we generated GFP reporter constructs bearing the upstream region fused to the first introns from both light (U53) and dark (U76) alleles and measured reporter protein activity in various tissues (Fig. 4 and fig. S7). In the developing head (Fig. 4, B and C), legs (Fig. 4, D and E), larval brain (Fig. 4, F and G), wing (Fig. 4, H and I), and haltere (Fig. 4, J and K), both light and dark regulatory regions displayed similar amounts of activity (fig. S7V). However, in the abdomen, we observed a pronounced 83% reduction in activity of the dark allele regulatory region relative to that of the light allele (17 ± 3%) (Fig. 4, L and M, and fig. S7V). This decrease is very similar in magnitude to the reduction in *ebony* mRNA expression in the dark lines (Fig. 2). Thus, mutations in the dark line regulatory region affect gene expression with a high degree of spatial specificity and provide direct evidence that the modular architecture of cis regulatory regions minimizes the pleiotropic effects of functional mutations.

Multiple functional mutations underlie ebony enhancer evolution. To identify the position, number, kind, and size of effects of functionally relevant mutations within the *ebony* abdominal enhancer, we compared dark U76 and light U62 alleles because these represent the two extremes of *ebony* expression. Between the U76 and the U62 alleles, there are ~120 nucleotide differences scattered over the 2.4-kb abdominal enhancer [44 point mutations and 76 base pairs (bp) differing because of 10 insertions or deletions (indels)] that could potentially contribute to the observed difference in activity. To localize functional differences, we first created chimeric reporter constructs with groups of mutations and then narrowed these to individual changes that contribute to the activity of chimeric constructs. Our analysis below suggests that a minimum of five mutations differentiate the activities of dark and light lines, two of which are specific to the dark haplotype.

We focused on a 2.4-kb region that contained the 0.7-kb core abdominal element ("abd" in Fig. 4A) and recapitulated the difference in RNA expression between dark (U76) and light (U62) lines, such that the dark allele construct expressed 22% of the reporter activity of the light allele construct (fig. S8, B and C). We subdivided the 2.4-kb region into three subregions (X, Y, and Z, Fig. 5A) and systematically substituted individual fragments from the light allele into the dark allele construct. Of the three subregions tested, the Z fragment showed the strongest effect (fig. S8D), increasing reporter activity from 22% to 67% of the activity of the light allele. Moreover, in the reciprocal construct, swapping in the Z fragment was sufficient to decrease activity of the light allele from 100% to 46% activity (fig. S8E).

Several previously identified candidate mutations were only observed on the dark haplotype, the majority of which (five out of eight) map to the 2.4-kb regulatory region (fig. S8A, red bars labeled "Dark Specific Substitutions"). Replacement of all five substitutions in the dark allele construct with the nucleotides present in the light allele increased reporter activity to 70% of that of the light allele construct, demonstrating that they include functionally important mutations (fig. S8F). The Z fragment contains four of the five dark-specific mutations within the 2.4-kb element (fig. S8A), so we reverted the individual dark-specific substitutions of the dark allele construct. Dark-specific substitutions 2 and 3 showed no effect on the level of reporter expression (table S2), whereas substitution 4

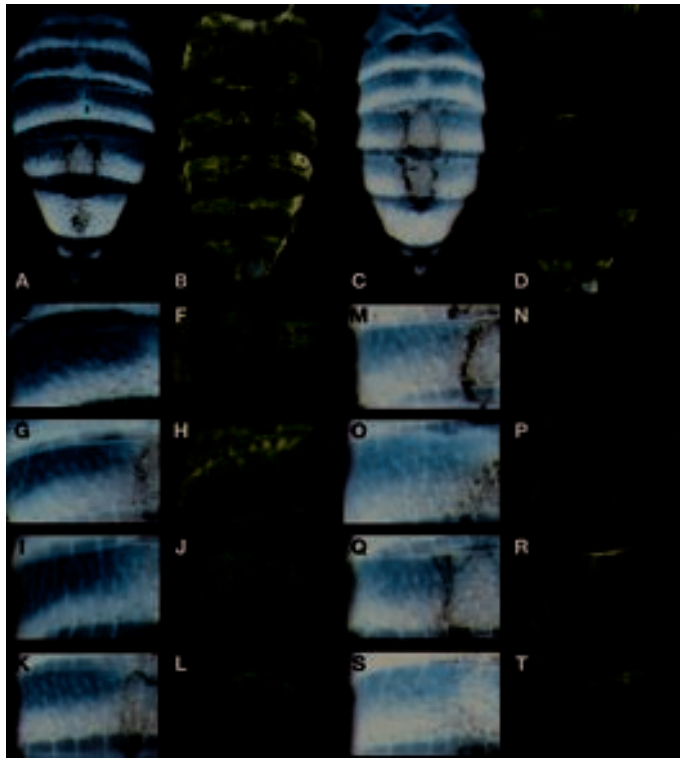

Fig. 2. *ebony* expression correlates with abdominal pigmentation within the Ugandan population. Abdominal pigmentation phenotypes of U53 (**A**) and U76 (**C**). The region outlined in (A) marks the A4 hemitergite imaged in (**E** to **T**). Accumulation of ebony transcript in the abdomen of U53 (**B**) and U76 (**D**) flies within 1 hour after eclosion was revealed by in situ hybridization. The developing U76 fly (C) shows greatly reduced amounts of *ebony* mRNA throughout the abdomen (D). [(E), (G), (I), (K), (M), (O), (Q), and (S)] Images of A4 hemitergite, as outlined in (A), from eight lines. [(F), (H), (J), (L), (N), (P), (R), and (T)] The corresponding amount of *ebony* mRNA expression within 1 hour post-eclosion revealed by in situ hybridization. Alleles are as follows: for (E) and (F), U53; (G) and (H), U62; (I) and (J), U64; (K) and (L), U65; (M) and (N), U75a; (O) and (P), U75b; (Q) and (R), U76; and (S) and (T), U78.

showed a small effect on expression, raising activity from 22% to 35% (fig. S8G). Substitution 5, however, caused a dramatic increase to 64% of the light allele activity (fig. S8H). Therefore, at least two novel substitutions in the Z fragment have contributed to the divergence of the dark and light haplotypes, with substitution 5 providing the largest effect.

To account for the remaining ~50% difference in activity, we turned to the X and Y fragments. No contribution of the X fragment (which contained dark-specific substitution 1) was observed when the light allele X fragment was swapped into the dark allele construct (fig. S8I). However, the chimeric construct bearing the Y fragment from the light line increased activity from 22% to 47% (fig. S8J), demonstrating that one or more functional mutations exist in the Y fragment. The Y fragment encompasses the core abdominal activity, the smallest span of DNA sufficient to drive strong reporter expression in the abdomen (figs. S6 and S8A). Comparison of the isolated Y fragment activities of the light and dark alleles also revealed much weaker activity of the dark allele Y fragment construct (25% relative to light) (fig. S9, B and C).

In order to pinpoint causative mutations within the Y fragment, we assayed a series of Y fragment GFP reporter constructs. Twenty-five point mutations and four indels (encompassing 42 bp) exist between the light U62 and dark U76 alleles Y fragment sequences. The major contribution to expression differences (81%) mapped to the 5′ half of the Y fragment (fig. S9, D and E), which allowed us to narrow the 67 candidate nucleotides down to the eight point mutations that differ in this region of the Y fragment (Fig. 5B). Of these eight candidates, three were eliminated because they were found in other strongly expressing Y fragments. We reverted each of the five remaining candidate substitutions individually from the dark allele to that present in the light allele. Mutations at positions 27 and 32 increased dark allele Y fragment activity from a 25% baseline to 54% and 50%, respectively, of the light allele Y fragment activity (fig. S9, F and G). The third substitution at position 137 had a more dramatic effect on the Y fragment activity, raising expression to 80% of light Y fragment expression (fig. S9H) (note that the sum of effects exceeds 100%, so individual effects are not strictly additive). These results suggest that at least three substitutions within the Y fragment contributed to the overall reduction of abdominal enhancer activity.

The five mutations that functionally differentiate the dark and the light haplotypes cause a decrease in the activity of the dark allele enhancer. The mutation with the greatest effect arose at a considerable distance (270 bp) from the core element. If this mutation is in an activator binding site, we would expect that this sequence would lie in the core element. Alternatively, the mutation may represent a repressor binding site. Indeed, when we deleted this site and the five adjacent nucleotides 5′ and 3′ to it, the enhancer drove a dramatic increase in reporter expression, from 22% to 106% of the light haplotype activities (fig. S8L). The greater effect of deleting these sites relative to reverting the nucleotide raised the possibility that these sites serve a function in the light allele. When we engineered the identical deletion into the light haplotype, reporter activity also increased (fig. S8M, 170% of light haplotype), indicating that this sequence is required to repress enhancer activity and that the substitution in the dark haplotype further repressed *ebony* expression.

Together, these data show that multiple mutations (at least five), with varying effects (accounting for 8% to 40% of the overall difference in activity) and representing different kinds of functional change (reduced activation strength, increased repression), underlie the evolution of the *ebony* abdominal enhancer.

Adaptive evolution via standing variation and new mutations. The observation that dark-specific substitutions accounted for a subset of the causative mutations raised the possibility that the path of *ebony* enhancer evolution involved both new mutations (the shared dark-specific substitutions) and standing variation (Fig. 5B). To assess the potential origins of the five substitutions, we examined the enhancer sequences of lines obtained from various regions in Africa (Fig. 5C).

The three causative substitutions located in the Y fragment occurred at high frequency in both light lines of the Ugandan population and in the light Kenyan population sample (Fig. 5B) and are also found in very distant African populations (Fig. 5C). Two of the substitutions were observed in all five populations sampled. The third Y fragment substitution was found in four of the five populations. These results demonstrate widespread standing genetic variation at the relevant sites in the Y fragment of the *ebony* abdominal enhancer.

The dark-specific substitutions were not observed in any other lines from Kenya or Uganda. Among 67 endemic fly lines from five African regions examined in our survey, the only other location where dark-specific mutations (numbers 4 and 5) occurred was in nearby Rwanda and was associated with the dark haplotype (Fig. 5C). The absence of these substitutions in isolation across the ancestral range of *D. melanogaster* indicates that they either arose de novo or were rare variants present in the population when the dark haplotype was selected.

The existence of both common polymorphisms and rare substitutions contributing functional changes to *ebony* expression raised the

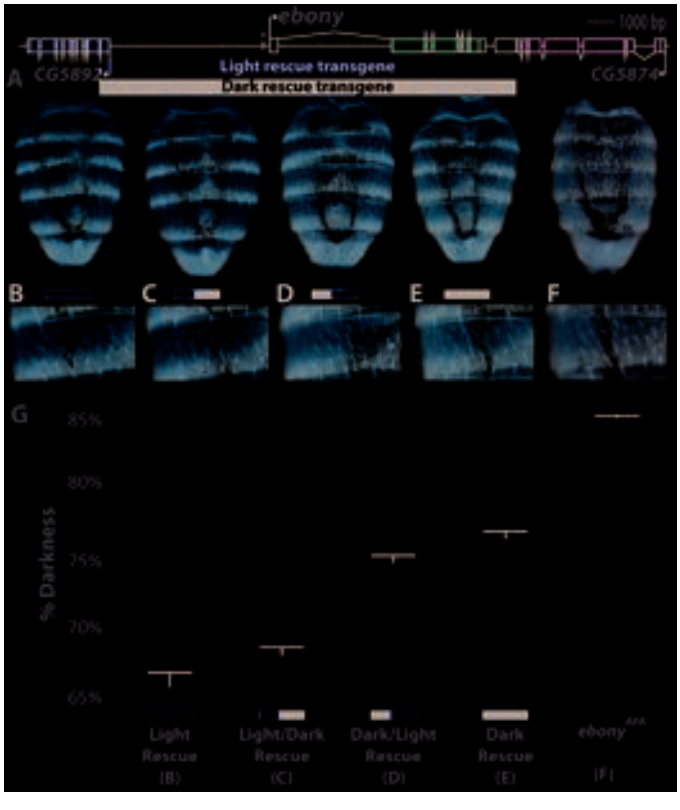

Fig. 3. Noncoding variation at *ebony* causes abdominal melanism. By using transgenic complementation, we localized abdominal pigmentation differences between light and dark *ebony* alleles to the 5′ noncoding region. (**A**) Schematic of the *ebony* gene, indicating the span of rescue transgenes tested. The asterisk denotes the location at which light/dark chimeric transgenes were fused. Rescue transgenes were transformed into *D. melanogaster* and crossed into an *ebony* null mutant background [(**F**), $ebony^{AFA}$]. (**B**) Rescue of the *ebony* mutant abdominal phenotype by one copy of a U62 (Light) *ebony* transgene. (**C**) Animal bearing one copy of a chimeric transgene consisting of the 5′ regulatory region from the light line and the transcription unit of the *ebony* gene of a dark line displays a light abdominal phenotype that is similar to the light line. (**D**) A fly bearing the dark line's 5′ regulatory region fused to the transcription unit of the light allele shows a dark phenotype that is similar to the dark line rescue transgene phenotype. (**E**) A rescue transgene derived from the dark line U76 complements the *ebony* mutation to a much lesser degree than the light line transgene. (**G**) Quantification of the amount of abdominal phenotypic rescue by transgenes. Letters below each column label correspond to the images above. Bars indicate standard error of the mean.

potential scenario that the relevant haplotype of standing variation in the Y fragment was assembled before dark-specific substitutions appeared and adaptive selection resulted in their high frequency. To test this scenario and to place these functional changes on a relative time scale, we took note of a Ugandan line (U65) that exhibited intermediate pigmentation (Fig. 1), *ebony* expression (Fig. 2, K and L), and abdominal enhancer activity (fig. S8K). Of all the nonmelanic lines examined, the Y fragment of U65 was most similar to the dark haplotype Y fragment, harboring all three functionally relevant Y fragment mutations (Fig. 5B) and sharing a ~1-kb region of sequence similarity with the dark line haplotype.

Within the 0.9-kb tract of polymorphisms shared between U65 and the dark strain haplotype, four mutations have arisen that differentiate the two, allowing us to estimate that they shared a common ancestor about 395,000 generations ago (SOM text). In contrast, the dark haplotype has accumulated just three substitutions across 14 kb among four lines, suggesting that these four alleles last shared a common ancestor only about 9000 generations ago. The 95% confidence intervals for these estimates do not overlap, which allows us to infer that the Y fragment haplotype existed long before the dark-specific substitutions arose (fig. S10). Hence, we have resolved two steps in the evolution of this adaptation: the assembly of functional standing variation followed by the recent addition of beneficial dark-specific substitutions that resulted in the full decrease of *ebony* expression, caused pronounced abdominal melanism, and which were swept to high frequency (fig. S11).

The genetic path of enhancer evolution. We have shown that the adaptive evolution of melanism in a Ugandan population of *D. melanogaster* occurred through multiple, stepwise substitutions in one enhancer of the *ebony* locus. We suggest that this genetic path of enhancer evolution with multiple substitutions of varying effect sizes, which originate from both standing variation and new mutations and combine to create an allele of large effect, may be a general feature of enhancer evolution in populations. This view is consistent with studies that have demonstrated that substitutions at multiple sites within enhancers are responsible for evolutionary changes in gene expression (*6*, *7*, *19*–*22*).

The pattern of multiple substitutions in enhancers also makes sense in light of their functional organization. Enhancers contain numerous transcription factor binding sites that are broadly distributed across a few hundred base pairs or more, all of which contribute to overall transcriptional output. Variation in enhancer output can and does arise from modifications at any of a large number of sites, and functional standing variation in enhancers is abundant in populations (*23*, *24*).

Enhancers and proteins are very distinct macromolecular entities, and it is useful to consider

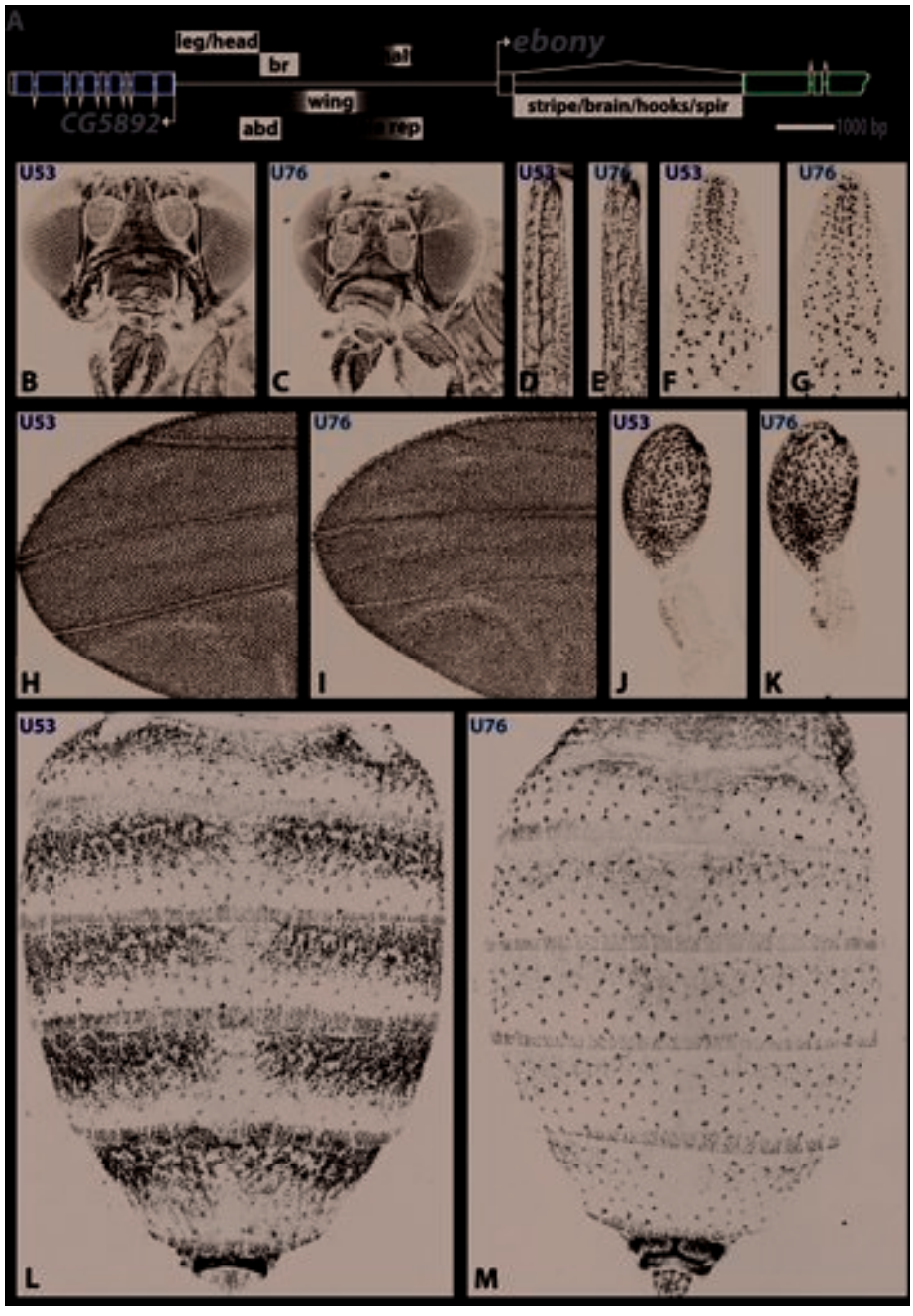

Fig. 4. The divergence in *ebony* activity is confined to a modular enhancer. Localization of *ebony* regulatory sequences in a GFP reporter assay; the difference in activity between light and dark alleles is restricted to the abdomen. (**A**) Map of ebony locus displaying the location of enhancers mapped through reporter assays. Black bars denote regions required for activity, whereas gray areas delineate the area in which enhancer boundaries lie. br indicates bristles; male rep, male repression; halt, haltere; stripe, abdominal tergite stripe repression; brain, third instar larval brain; hooks, larval mouth hooks; and spir, larval spiracles. (**B** to **M**) Reporter activity driven by the complete regulatory region of the *ebony* locus from a light [U53 in (B), (D), (F), (H), (J), and (L)] or dark [U76 in (C), (E), (G), (I), (K), and (M)] chromosome extraction line. Shown in (B) and (C) is the head; (D) and (E), femur of T2 legs; (F) and (G), third instar brain; (H) and (I), wing; (J) and (K), haltere; (L) and (M), adult abdomen. Staging and fluorescence quantification are presented in SOM text.

the potentially different constraints operating on enhancers and proteins that might affect their evolutionary trajectories. At least five constraints limit variation within proteins and restrict the path of protein evolution. The first constraint is pleiotropy. Coding mutations in pleiotropic genes will generally affect all functions, which will most likely be deleterious. The second constraint is the triplet genetic code that cannot accommodate most indels. Third, proteins must fold properly, and most random amino acid replacements are destabilizing and deleterious (*25*, *26*). Fourth,

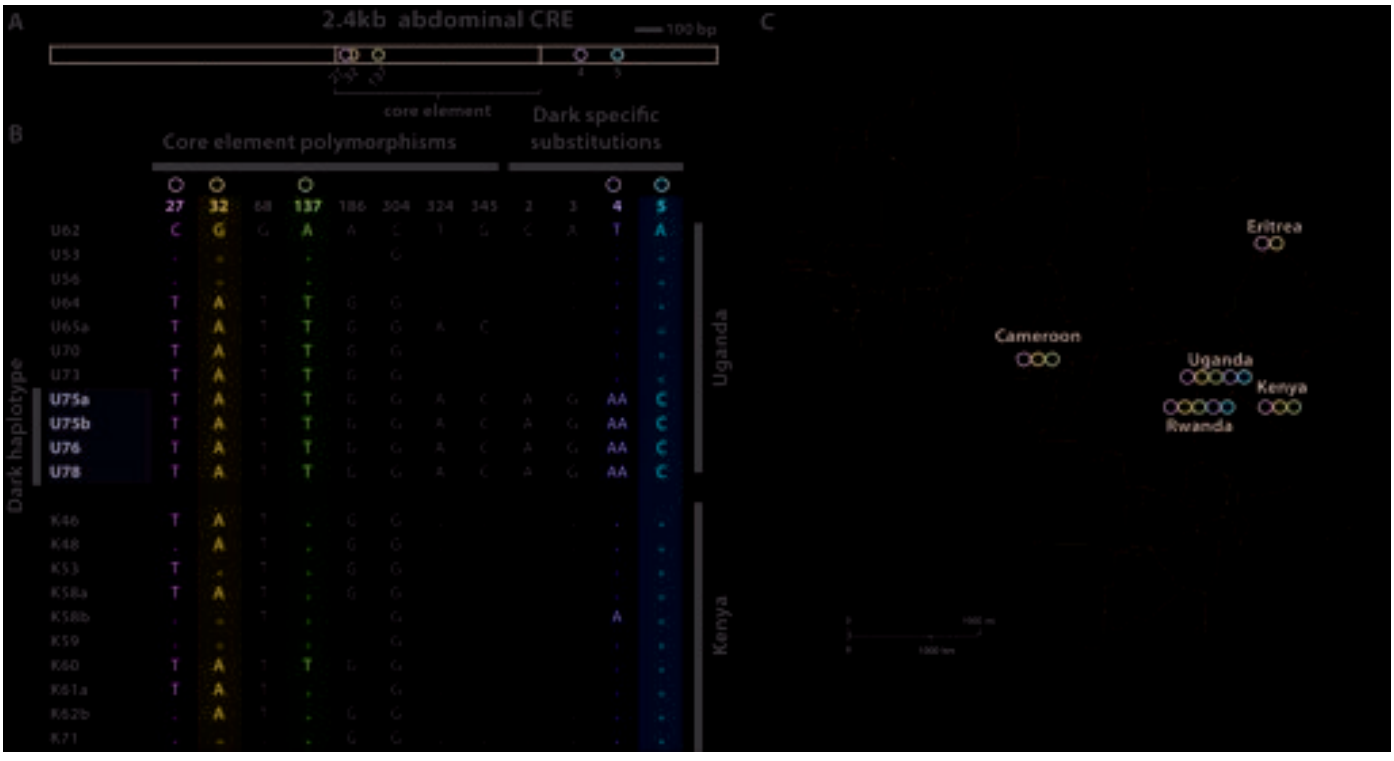

Fig. 5. Multiple mutations in the *ebony* abdominal cis regulatory element contribute to enhancer activity differences. Five mutations decrease ebony expression in the dark allele and show a varied distribution across Africa. (**A**) Schematic of *ebony* abdominal enhancer, showing the positions of the X, Y, and Z fragments and the relative position of identified causative mutations. (**B**) Candidate mutations in the core element and the dark-specific substitutions that were tested by reporter assay. Colored shading of residues highlights mutations with functional contribution to enhancer divergence. Numbers for core element substitutions correspond to the base pair position of each nucleotide within the minimal abdominal element. Numbers below dark-specific substitutions coincide with their order in the region of the abdominal element (see fig. S9 for a schematic representation). (**C**) Map of African continent displaying distribution of causative mutations identified in the study. The color coding for mutations corresponds to the shading and colored circles above each relevant mutation in (A).

because of demands on protein structure, the order in which specific amino acid replacements may occur is typically constrained (*13*, *14*), thus reducing the number of genetic paths adaptation may take. And lastly, many proteins often have a single active site or one or a few binding domains, such that changes at only a very limited number of positions may directly alter properties of these sites.

In contrast, more relaxed constraints appear to operate on evolving regulatory elements. The evolution of individual, modular enhancers circumvents the pleiotropic effects of coding mutations, and our results illustrate precisely why this is the case. Obviously, there is no triplet code, so a greater range of mutational events can be accommodated. Furthermore, enhancers are not constrained by three-dimensional structure; consequently, the order in which substitutions may occur would appear to be much less constrained. Indeed, we found many combinations of functionally relevant polymorphisms in our survey of *ebony* haplotypes. In addition, chimeric enhancers that placed more recent mutations in an ancestral context exhibited intermediate levels of function, as would be expected if multiple alternate genetic paths are viable. And lastly, because enhancers generally contain numerous binding sites for transcription factors distributed throughout their sequence, there may be more potential sites where substitutions may modify function. Here, we identified substitutions that both decreased activation and increased repression. Thus, during their respective paths of adaptation, enhancers may present a larger mutational target for functional modification and may have a greater number of possible genetic paths open to them relative to typical protein-coding sequences.

References and Notes

1. S. B. Carroll, J. K. Grenier, S. D. Weatherbee, *From DNA to Diversity: Molecular Genetics and the Evolution of Animal Design* (Blackwell, Malden, MA, ed. 2, 2005).
2. E. H. Davidson, *The Regulatory Genome: Gene Regulatory Networks in Development and Evolution* (Academic Press, Burlington, MA, 2006), p. xi.
3. N. Gompel, B. Prud'homme, P. J. Wittkopp, V. A. Kassner, S. B. Carroll, *Nature* **433**, 481 (2005).
4. B. Prud'homme *et al.*, *Nature* **440**, 1050 (2006).
5. S. Jeong, A. Rokas, S. B. Carroll, *Cell* **125**, 1387 (2006).
6. A. P. McGregor *et al.*, *Nature* **448**, 587 (2007).
7. T. M. Williams *et al.*, *Cell* **134**, 610 (2008).
8. C. J. Cretekos *et al.*, *Genes Dev.* **22**, 141 (2008).
9. S. Jeong *et al.*, *Cell* **132**, 783 (2008).
10. G. A. Wray, *Nat. Rev. Genet.* **8**, 206 (2007).
11. S. B. Carroll, *Cell* **134**, 25 (2008).
12. D. L. Stern, V. Orgogozo, *Evolution* **62**, 2155 (2008).
13. E. A. Ortlund, J. T. Bridgham, M. R. Redinbo, J. W. Thornton, *Science* **317**, 1544 (2007); published online 15 August 2007 (10.1126/science.1142819).
14. D. M. Weinreich, N. F. Delaney, M. A. DePristo, D. L. Hartl, *Science* **312**, 111 (2006).
15. J. T. Bridgham, E. A. Ortlund, J. W. Thornton, *Nature* **461**, 515 (2009).
16. J. E. Pool, C. F. Aquadro, *Mol. Ecol.* **16**, 2844 (2007).
17. A. Richardt *et al.*, *J. Biol. Chem.* **278**, 41160 (2003).
18. P. J. Wittkopp, J. R. True, S. B. Carroll, *Development* **129**, 1849 (2002).
19. S. Prabhakar *et al.*, *Science* **321**, 1346 (2008).
20. M. V. Rockman *et al.*, *PLoS Biol.* **3**, e387 (2005).
21. S. A. Tishkoff *et al.*, *Nat. Genet.* **39**, 31 (2007).
22. L. C. Olds, E. Sibley, *Hum. Mol. Genet.* **12**, 2333 (2003).
23. D. J. Verlaan *et al.*, *Genome Res.* **19**, 118 (2009).
24. P. J. Wittkopp, B. K. Haerum, A. G. Clark, *Nat. Genet.* **40**, 346 (2008).
25. J. D. Bloom, S. T. Labthavikul, C. R. Otey, F. H. Arnold, *Proc. Natl. Acad. Sci. U.S.A.* **103**, 5869 (2006).
26. J. D. Bloom *et al.*, *Proc. Natl. Acad. Sci. U.S.A.* **102**, 606 (2005).
27. The GenBank accession numbers for the sequences reported in the paper are GU108024 to GU108150.

28. We thank H. Dufour and T. Williams for discussions and comments on the manuscript and K. Vaccaro for technical assistance. This work was supported by NIH postdoctoral fellowships F32GM78972 (M.R.) and F32HG004182 (J.E.P.), NIH grant GM036431 (C.F.A.), and the Howard Hughes Medical Institute (S.B.C.).

Supporting Online Material

www.sciencemag.org/cgi/content/full/326/5960/1663/DC1
Materials and Methods
SOM Text
Figs. S1 to S11
Tables S1 to S4

29 June 2009; accepted 15 October 2009
10.1126/science.1178357

www.sciencemag.org/cgi/content/full/326/5960/1663/DC1

Supporting Online Material for

Stepwise Modification of a Modular Enhancer Underlies Adaptation in a *Drosophila* Population

Mark Rebeiz, John E. Pool, Victoria A. Kassner, Charles F. Aquadro, Sean B. Carroll*

*To whom correspondence should be addressed. E-mail: sbcarrol@wisc.edu

Published 18 December 2009, *Science* **326**, 1663 (2009)
DOI: 10.1126/science.1178357

This PDF file includes:

Supporting Online Material

Genetic association of pigmentation phenotypes of the dark Ugandan lines with variation at the *ebony* locus

The contribution of *ebony* genetic variation to pigmentation differences was examined by analyzing haplotypes within the region containing the identified causative mutations, using a standard analysis of variance (ANOVA). The 11 sequenced Uganda alleles represent five distinct haplotypes within this region. After performing basic ANOVA, the proportion of phenotypic variance explained by these five allelic categories was estimated as:

$$\hat{\omega}^2 = \frac{SS_{hap} - df \cdot MS_{error}}{SS_{total} + MS_{error}},$$

where SS_{hap} is the sum of squares between haplotypes, SS_{total} is the total sum of squares, df is the degrees of freedom, and MS_{error} is the mean square error. Based upon the analysis of the 11 haplotypes, we estimate that variation at *ebony* contributes approximately 83% of the difference in pigmentation between haplotypes. The analysis was also repeated to compare the haplotype of the darkest four alleles against all others and we obtained an estimate that *ebony* contributed 50% of the difference in phenotype. By basing our estimate only on this portion of the *ebony* regulatory region, and by simplifying the data to haplotypes, we may underestimate the total contribution of *ebony* variation to A4 pigmentation score. However, this analysis is sufficient to establish that *ebony* is the major contributor to pigmentation differences among the Uganda third chromosome lines studied here.

Estimates of allele divergence times

We infer that the dark-specific substitutions, which generated pronounced melanic pigmentation by reducing *ebony* expression in the abdomen, achieved this phenotypic change only by occurring on a specific allelic background with respect to the adjacent core abdominal element. Outside of the melanic lines, this core element allele is most closely represented in the current data set by U65, and it appears to have

persisted as standing genetic variation. Unlike the haplotypes of the darkest four lines, which share nearly identical sequences across >14kb (suggesting positive selection;(*1*)), the shared sequence between U65 and the melanic alleles spans less than 1kb (which is more typical of the scale of haplotype sharing at selectively neutral loci in this population;(*2*)).

Furthermore, an analysis of allelic divergence times (see Methods below) indicates that U65-like core element alleles existed prior to the adaptive event that elevated the melanic mutations and its extended haplotype to high frequency. The darkest four lines share nearly identical haplotypes across 14,386 bp. Within this region, only three new substitutions (each observed only on one of these four chromosomes) appear to have arisen since the divergence of these alleles. Based on this data, we estimate that these four alleles share a common ancestor 8,989 generations ago (*3*), with a 95% confidence interval of 1,854 to 26,269 generations. For the sequence shared between U65 and the melanic alleles, we conservatively tried to include as many sites with as few unique mutations as possible (to reduce the estimated coalescence time). The 873 bp region defined by these criteria included four mutations on either the U65 or the melanic lineage. The divergence time between these lineages was estimated at 394,992 generations ago, with a 95% confidence interval of 107,625 to 1,011,336 generations.

Based on the non-overlapping confidence intervals obtained above, we infer that the U65 abdominal element allele did not evolve from the melanic alleles via recombination, because this scenario would not allow enough time for the mutations that differentiate U65 and the melanic alleles to occur. Instead, it appears that a class of abdominal element haplotypes similar to that of U65 and the melanic alleles was present before positive selection acted on the dark mutations' haplotype. Combining this inference with the observation that the melanic mutations' phenotypic impacts are dependent upon linked variation at the adjacent abdominal core element, it appears that the melanic mutations needed to occur (via *de novo* mutation or recombination) on a specific haplotype in order to have a strong effect on pigmentation. In terms of gene expression, we suggest that the melanic mutation of largest effect represents an increase of repression, but has only a minor effect unless combined with a weakened version of the core abdominal element.

Materials and Methods

Fly Stocks

The third chromosome extraction lines used in the study were described in (*1*). Briefly, individuals from isofemale lines were crossed through a series of balancers such that their X chromosome was of cosmopolitan origin, and their third chromosome was a homozygous chromosome from the isofemale line. While second chromosomes may have mixed origins in these lines, the second chromosome was found to have no effect on pigmentation in this population (*1*).

DNA sequencing

DNA sequence data for 10 Uganda third chromosome lines was collected for a series of flanking loci: 15, 30, 100, and 200 kb upstream and downstream from the originally sequenced 20 kb block. Loci ~1 kb in length were amplified using a standard polymerase chain reaction and sequenced using an ABI 3730 capillary sequencer. Identical haplotypes were identified at each locus, to facilitate comparison with the previous data.

Additional sequence data was also obtained for a ~1 kb region containing the causative variants implicated in this study, in a larger sample of African third chromosome lines. The samples represented in this data are described in Pool and Aquadro (2006), and include lines from Cameroon (15 lines from the CD, CN, CO, and CW samples), Eritrea (9 lines), Rwanda (4 lines), and Uganda (14 previously unsequenced lines).

Adult abdominal phenotypes

Adult cuticular images were collected on a Olympus SZX16 Zoom Stereo Microscope equipped with an Olympus DP71 microscope digital camera. Flies were imaged at 8-25 days post-eclosion, and not exposed to CO_2 to avoid tanning effects. We found very little difference in pigmentation score between younger flies (8days, "extraction lines" in fig S2A) and older flies (20-25 days, "extraction lines" in fig. S2B). To measure the mean darkness of F2 progeny, extraction lines, and transgenic complementation lines, images were converted to grayscale in Photoshop, and with the freehand selection tool, the anterior portion of each tergite was selected to obtain the grayscale darkness value that lies on a 0-255 scale. Percent-darkness was calculated as :

(255-grayscale darkness)/255 x 100.

in situ hybridization

in situ hybridization was performed as previously described, following the protocol available on the Carroll lab website (http://www.molbio.wisc.edu/carroll/methods/methods.html)(*4*). Flies were dissected within 30 minutes of eclosion. Abdominal samples were probed with a 2.1 kb digoxygenin riboprobe covering a portion of the coding region (primers 5'-AGCAGCTTCTTCGACTAT-3' 5'-GCTTACAACTAGTCAACA-3'). Alkaline phosphatase staining was developed in parallel, for an identical duration. After mounting on slides in a glycerol solution, abdomens were imaged on an Olympus SZX16 Zoom Stereo Microscope. To estimate relative expression levels, each image was quantified in Photoshop by setting the image to grayscale, and selecting the anterior two thirds of the tergite corresponding to a region that normally expresses *ebony* (i.e. Fig 2F). From this selection, intensity was scored on a scale from 0 to 255. Background intensity of the unstained abdominal tissue was calculated by measuring the posterior one third of each tergite (a region that doesn't express noticeable levels of *ebony* post-eclosion), and subtracting this value from the intensity of the anterior tergite measurement.

Reporter constructs and transgenic fly production

GFP reporters were constructed in the vector pS3AG as previously described (*5*). Sequences were curated in the GenePalette software package (*6*). Primers used to dissect the *ebony* regulatory region are shown in Table S4. All constructs were cloned into pS3AG using *Asc I* and *Sbf I* restriction sites. Segments of DNA from within the regulatory region were amplified from the lab strain Canton S. For the test of modularity experiments, the intron of ebony was placed downstream of GFP using an adjacent *Spe I* site. For *Spe I* insertions, the native orientation of the intron was maintained. All mutations and chimeras were generated by overlap extension of the existing 2.4 kb abdominal CRE and 0.7 kb core element constructs, with the exception of core mutations 27 and 32, which were introduced by modifying the core element forward primer. Primers used for generating mutant constructs are shown in Table S5.

Site-specific integration of transgenes was accomplished by injection of embryos containing a chromosomal source of ϕC31 integrase with a suitable landing site on the

second chromosome (51D) (*7*). For a majority of the transgenic lines, both landing site and construct identity were confirmed by diagnostic PCRs and sequencing of pS3AG inserts in single transgenic flies. To confirm landing sites, a PCR was performed that established the continuity of the 51D site with the acceptor minos insertion [M{3xP3-RFPattP'}] (5'-TCATCAGCGGTAGTATCTGCTCAG-3', 5'-CCGTTCCTTCCATGCGAACCTT-3'). To verify the construct inserted in transgenic lines, the insert was PCR amplified (5'-CACATGTGCAAGAGAACCCAGTG-3', 5'-CTGCGCTTGTTTATTTGCTTAGC-3') from a single fly (*8*).

Rescue Constructs

Constructs containing the entire *ebony* locus were amplified using the low-error polymerase phusion (NEB) in two steps. Fragment 1 was amplified (5'-TTCCGggcgcgccTTCACTCACTCTCCCACTGACTCCCA-3', 5'-TTGCCcctgcaggCCTGCTCTTAMAGCCSCTGCAATTAC-3'), and inserted into pS3AG using *Asc I* and *Sbf I* sites included in the primers (lowercase letters). Fragment 2 was amplified (5'-TTCCGggcgcgccTGCCAATTAGTGAGTGAGGGGACG-3', 5'-TTCCgcggccgcGCTGCAACTGGTTTGTGCGTATATGG-3'**)**, and cloned into pGEMT-Easy (Promega). To merge the two fragments, a convenient Acc65 I site located just upstream of the promoter was used (* in Fig 4A). The Fragment-1-pS3aG vector was cut with *Acc65 I* and *Not I*, yielding an acceptor plasmid that lacked GFP. Fragment-2 was cut out of pGEMT-Easy with *Acc65 I* and *Not I* (lowercase sequences included in the Fragment 2 primers), and was ligated into the Fragment 1-pS3aG vector. These cloning steps were carried out in parallel for both U62 and U76 *ebony* loci. Chimeric constructs were made by switching fragments at the *Acc65 I*/*Not I* ligation steps.

Constructs were then intergrated into the 51D landing site on the second chromosome using the same ϕC31 integrase system as the reporter constructs. Transgenic lines, each bearing a rescue construct on the second chromosome (51D landing site) were crossed through a series of balancers to generate transgenic flies homozygous for the *ebony* null allele e^{AFA}. Two independent lines of each construct were measured, and their data merged, as described in "Adult Abdominal Phenotypes". Similarly, transgenes were crossed through balancers to third chromosome extraction lines to generate transgenic flies homozygous for an extraction line.

To test the ability of light and dark rescue transgenes to complement the phenotype of the third chromosome extraction lines, a series of balancer crosses were

performed. Briefly, transgenic lines (inserted on the second chromosome) were crossed to a TM6B third chromosome balancer stock, males of the genotype:[w^-;*ebony* transgene; +/TM6B] were crossed to third chromosome extraction line females. Flies heterozygous for the transgene and extraction chromosome [w^-;*ebony* transgene/+; extraction/TM6B] were self-crossed, and progeny homozygous for the extraction line, carrying one copy of the transgene were selected based on eye color, and the lack of TM6B, and scored for pigmentation. Non-transgenic extraction line homozygote progeny from the same cross were used in this experiment to measure the pigmentation of the extraction lines alone.

Measurement of relative fluorescent intensity

Relative fluorescent activities of GFP reporters were determined as previously described with minor modifications (*4, 5*). All constructs compared were inserted into the same genomic context (51D) to eliminate position effects. For each construct, two lines were measured, and several abdomens of similar age (4 hours post-eclosion) were imaged. Legs, wings, and head were removed from each imaged fly, and placed in a well of Halocarbon 27 oil contained by 5 layers of double-sticky tape, and covered with a coverslip. Confocal maximum projections were collected on an Olympus Fluoview FV 1000 confocal microscope. Abdomens were imaged with standardized settings such that the brightest images were not saturated. The mean fluorescent intensity of an A4 hemitergite was measured using the ImageJ software package (http://rsbweb.nih.gov/ij/). Background signal was measured from a patch of tissue at the midline of the A4 tergite, where only bristle GFP expression is observed. Once background was subtracted from the A4 signal, the mean of several flies across two or more lines was ascertained, and expressed as percent activity relative to the light allele (U62) construct. Separate settings were used for Y Fragment and 2.4 kb abdominal CRE reporters. Effect sizes were calculated as the difference in relative expression between a mutant construct and the dark allele construct. For Y fragment constructs, effect sizes were normalized by the total effect of placing the light Y fragment into the dark 2.4 kb reporter (47% - 22% = 25%). Thus the maximum normalized effect size of any Y fragment mutation was 25%.

To measure the modular effects of the different alleles on different tissues, abdomens were imaged at 24 hours post-eclosion (to avoid pupal expression as well as expression from internal organs). Wings were imaged shortly after eclosion, after wings

had expanded. Head, legs, halteres , and bristles were measured 14-16 hours after eclosion. Larval structures (brain, mouth hooks, spiracles) were fixed for 15 min in PBS containing 4% paraformaldehyde before mounting and imaging in a glycerol mounting solution. For each tissue (except the wing), a region in the specimen that lacked nuclear GFP was measured in order to subtract background fluorescence.

Calculation of allelic divergence times

Allelic divergence times were estimated according to the method of Slatkin and Hudson (1991). Estimates were obtained for (a) the divergence time of the darkest four alleles, and (b) the divergence time between the core abdominal element alleles of U65 and the lineage represented by the darkest four alleles. In the case of (a), this analysis involves the assumption of a star phylogeny, which is considered valid in the case of positive selection, and is also supported by the lack of any mutations shared by just two of the four alleles. We consider case (b) to be an analysis of two lineages – U65 and the melanic lineage – because there are no mutational differences among the melanic alleles within this region.

Divergence time can be estimated according to the formula:

$$T = \frac{(\#\ \text{of mutations})}{(\#\ \text{of lineages} \times \text{length of region} \times \text{mutation rate})}$$

Confidence intervals on these estimates were obtained by treating the number of mutations as the observation from a Poisson process. The confidence interval for the expected number of mutations can then be obtained using standard χ^2 distributions (*9*), and this confidence interval for the expected number of mutations can be converted into a confidence interval for divergence time by using the formula shown above.

We used an estimate of 5.8×10^{9} mutations per bp, per generation (*10*), and so our estimate of *T* is given in terms of generations (rather than years). This estimate is based on mutation-accumulation lines, and may thus include mutations that would not persist even at low frequency in nature. However, using a lower mutation rate would simply rescale our results by a constant factor, and since our analysis focuses on the comparison of two estimates, this should not be a relevant concern.

For the analysis of U65 and the melanic lineage, there were several sites which clearly showed a window of common ancestry between these lineages without intervening recombination events, based on mutations shared only by these five sequences. In order to include the maximum number of shared sites (yielding a

conservatively lower estimate of divergence time), this window was extended until it reached sites showing clear evidence of recombination. These were sites in which U65 and the melanic lines had different alleles, and each of these alleles were present in other sequenced individuals, implying that the U65 and the melanic sequences were no longer closest relatives at these sites. A slight complication involved the apparent gene conversion event involving U78 in the upstream portion of this region. However, the boundaries of this gene conversion tract were easily identifiable, and its effects were clearly separable from the mutational history of the melanic lineage.

In an expanded sample of sequence variation among 67 sub-Saharan chromosomes, no extended haplotype identity was observed involving U65-like alleles. However, a short stretch of sequence identity was observed between the melanic/U65 abdominal element haplotype and a single allele from Eritrea, extending over just the *3'* 236 bp of this 367 bp element. The existence of this allele 1750km from the Uganda sample, in a sample where the full haplotype of the dark alleles was not observed, provides an additional suggestion that U65-like abdominal element alleles have segregated neutrally in sub-Saharan *D. melanogaster*.

References

1. J. E. Pool, C. F. Aquadro, *Mol Ecol* **16**, 2844 (Jul, 2007).
2. J. E. Pool, C. F. Aquadro, *Genetics* **174**, 915 (Oct, 2006).
3. M. Slatkin, R. R. Hudson, *Genetics* **129**, 555 (Oct, 1991).
4. S. Jeong *et al.*, *Cell* **132**, 783 (Mar 7, 2008).
5. T. M. Williams *et al.*, *Cell* **134**, 610 (Aug 22, 2008).
6. M. Rebeiz, J. W. Posakony, *Dev Biol* **271**, 431 (Jul 15, 2004).
7. J. Bischof, R. K. Maeda, M. Hediger, F. Karch, K. Basler, *Proc Natl Acad Sci U S A* **104**, 3312 (Feb 27, 2007).
8. G. B. Gloor *et al.*, *Genetics* **135**, 81 (Sep, 1993).
9. K. Ulm, *Am J Epidemiol* **131**, 373 (Feb, 1990).
10. C. Haag-Liautard *et al.*, *Nature* **445**, 82 (Jan 4, 2007).

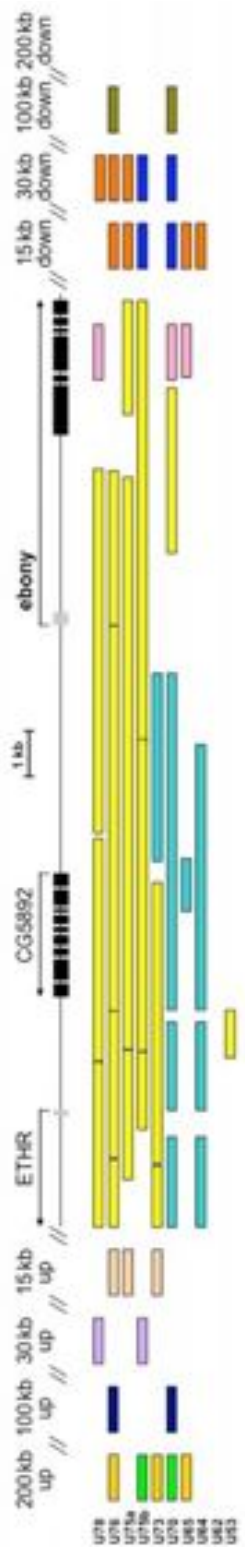
200 kb up
100 kb up
30 kb up
15 kb up
ETHR
CG5892
1 kb
ebony
15 kb down
30 kb down
100 kb down
200 kb down
U78
U76
U75a
U75b
U73
U79
U84
U82
U83

Figure S1

Figure S1. A partial selective sweep associated with abdominal melanism at *ebony*. Colored bars indicate haplotypes longer than 1 kb shared among 10 Uganda third chromosome lines. These lines are labeled and sorted according to A4 pigmentation score (left), revealing that the darkest four lines share a >14 kb block of identical haplotypes (yellow). Outside the central 20 kb fragment analyzed by Pool and Aquadro (2007), data from eight ~1 kb flanking loci confirm that the strongest signals of natural selection and genotype-phenotype association are localized within the *ebony* 5' regulatory region.

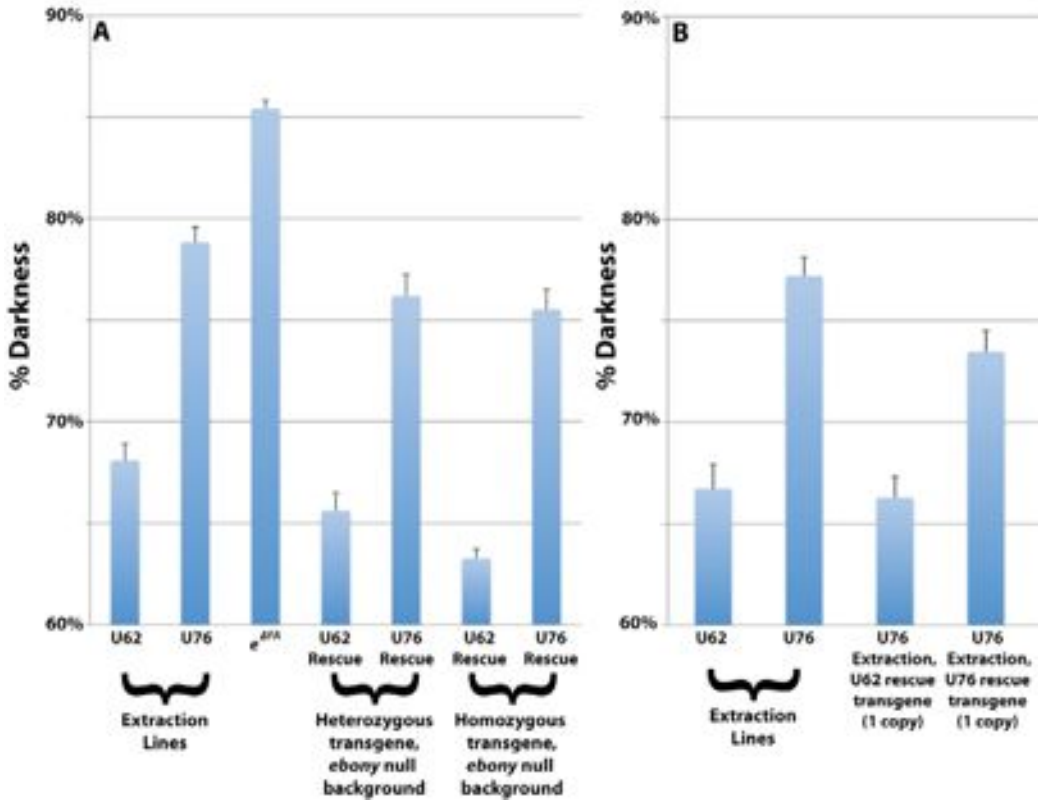

Figure S2. *ebony* is the major locus contributing to the dark phenotype of 3rd chromosome extraction lines. (A) Graph comparing the A4 pigmentation phenotype (% Darkness) of light and dark extraction lines to transgenic lines at 8 days post-eclosion. The difference in pigmentation between light (U62) and dark (U76) extraction lines is 10.6% darkness. e^{AFA} is an *ebony* null allele, resulting in a very dark melanic phenotype. Flies homozygous for e^{AFA}, carrying one, or two copies of *ebony* transgenes derived from U62 or U76 show a similar difference in pigmentation score (10.7% darkness for heterozygotes, 12.3% for homozygotes). (B) Graph depicting the phenotype of 25 day old animals homozygous for the dark (U76) third chromosomes complemented with one copy of the indicated *ebony* transgenes (U62 or U76) provided on the second chromosome. One copy of the light (U62) transgene in the background of the dark (U76) extraction line is sufficient to revert the dark phenotype to light. However, the dark (U76) *ebony* transgene, fails to fully complement the extraction line phenotype, causing some lightening of the cuticle, as expected for an animal bearing three copies of a gene with reduced function. Comparison of extraction lines at 8 days (A) yields similar pigmentation results as those obtained from older flies (B, compare the "extraction lines"). Phenotypes are measured as the percent of grayscale darkness of the fourth abdominal tergite. Error bars show S.E.M.

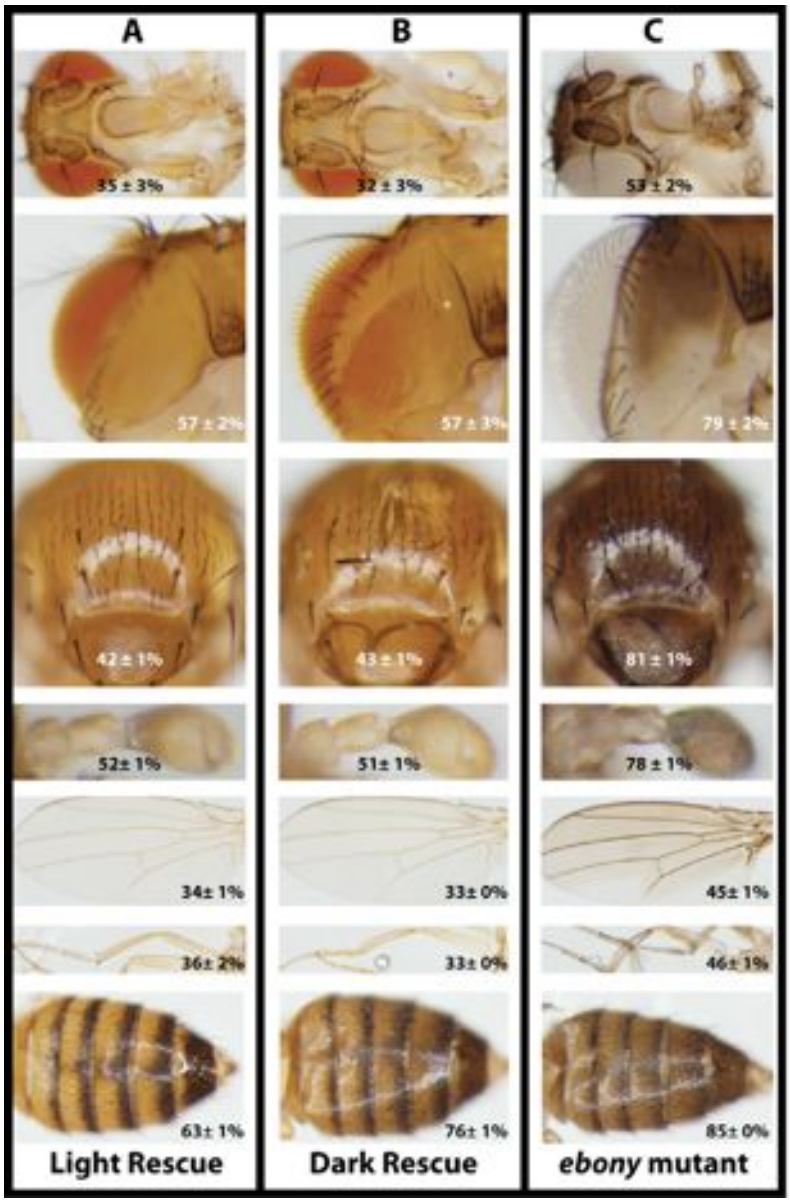

Figure S3. Mosaic complementation of *ebony* mutant phenotypes by wild derived rescue transgenes. Images show representative cuticular phenotype of 20-day old females homozygous for both an *ebony* null mutation (*ebony*^{AFA}), and two different *ebony* transgenes. (A) Phenotype of *ebony*^{AFA} mutant complemented by a U62 (Light) *ebony* rescue transgene. (B) An *ebony* transgene derived from the dark U76 fly line is able to rescue all cuticular phenotypes to a similar extent as U62, with the exception of the abdominal pigmentation phenotype. (C) phenotype of *ebony*^{AFA} mutation. Panels show images (from top to bottom) of the face, posterior head, thorax, haltere, wing, legs, and abdomens. Pigmentation score (% darkness) mean and S.E.M. are presented for each tissue.

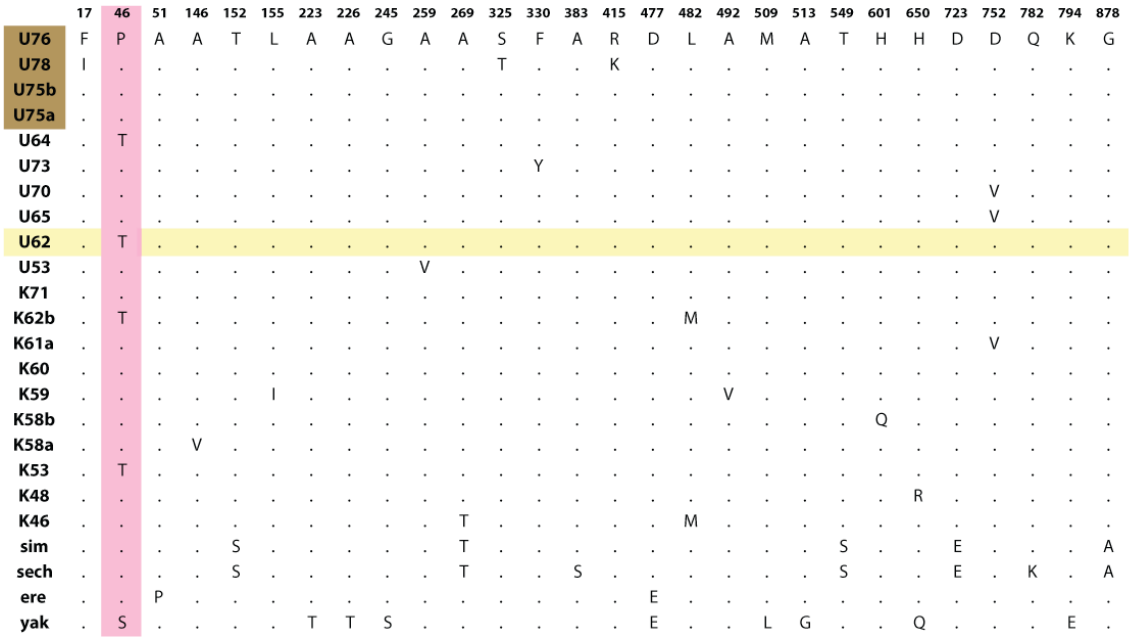

	17	46	51	146	152	155	223	226	245	259	269	325	330	383	415	477	482	492	509	513	549	601	650	723	752	782	794	878
U76	F	P	A	A	T	L	A	A	G	A	A	S	F	A	R	D	L	A	M	A	T	H	H	D	D	Q	K	G
U78	I	.	.	.	.	.	.	.	.	.	.	T	.	.	K	.	.	.	.	.	.	.	.	.	.	.	.	.
U75b	.	.	.	.	.	.	.	.	.	.	.	.	.	.	.	.	.	.	.	.	.	.	.	.	.	.	.	.
U75a	.	.	.	.	.	.	.	.	.	.	.	.	.	.	.	.	.	.	.	.	.	.	.	.	.	.	.	.
U64	.	T	.	.	.	.	.	.	.	.	.	.	.	.	.	.	.	.	.	.	.	.	.	.	.	.	.	.
U73	.	.	.	.	.	.	.	.	.	.	.	.	Y	.	.	.	.	.	.	.	.	.	.	.	.	.	.	.
U70	.	.	.	.	.	.	.	.	.	.	.	.	.	.	.	.	.	.	.	.	.	.	.	.	V	.	.	.
U65	.	.	.	.	.	.	.	.	.	.	.	.	.	.	.	.	.	.	.	.	.	.	.	.	V	.	.	.
U62	.	T	.	.	.	.	.	.	.	.	.	.	.	.	.	.	.	.	.	.	.	.	.	.	.	.	.	.
U53	.	.	.	.	.	.	.	.	V	.	.	.	.	.	.	.	.	.	.	.	.	.	.	.	.	.	.	.
K71	.	.	.	.	.	.	.	.	.	.	.	.	.	.	.	.	.	.	.	.	.	.	.	.	.	.	.	.
K62b	.	T	.	.	.	.	.	.	.	.	.	.	.	.	.	.	M	.	.	.	.	.	.	.	.	.	.	.
K61a	.	.	.	.	.	.	.	.	.	.	.	.	.	.	.	.	.	.	.	.	.	.	.	.	V	.	.	.
K60	.	.	.	.	.	.	.	.	.	.	.	.	.	.	.	.	.	.	.	.	.	.	.	.	.	.	.	.
K59	.	.	.	.	.	I	.	.	.	.	.	.	.	.	.	.	.	V	.	.	.	.	.	.	.	.	.	.
K58b	.	.	.	.	.	.	.	.	.	.	.	.	.	.	.	.	.	.	.	.	.	Q	.	.	.	.	.	.
K58a	.	.	.	V	.	.	.	.	.	.	.	.	.	.	.	.	.	.	.	.	.	.	.	.	.	.	.	.
K53	.	T	.	.	.	.	.	.	.	.	.	.	.	.	.	.	.	.	.	.	.	.	.	.	.	.	.	.
K48	.	.	.	.	.	.	.	.	.	.	.	.	.	.	.	.	.	.	.	.	.	.	R	.	.	.	.	.
K46	.	.	.	.	.	.	.	.	.	T	.	.	.	.	.	.	M	.	.	.	.	.	.	.	.	.	.	.
sim	.	.	.	.	S	.	.	.	.	T	.	.	.	.	.	.	.	.	.	.	S	.	.	E	.	.	.	A
sech	.	.	.	.	S	.	.	.	.	T	.	.	.	S	.	.	.	.	.	.	S	.	.	E	.	K	.	A
ere	.	.	P	.	.	.	.	.	.	.	.	.	.	.	.	E	.	.	.	.	.	.	.	.	.	.	.	.
yak	.	S	.	.	.	.	T	T	S	.	.	.	.	.	.	E	.	.	L	G	.	.	Q	.	.	.	E	.

Figure S4. The U76 *ebony* coding region contains no derived non-synonomous mutations. Alignment of all *ebony* coding sequences from Uganda and Kenya, compared to outgroup species, *D. sechellia* (sech), *D. simulans* (sim), *D. erecta* (ere), and *D. yakuba* (yak). Only one difference (pink shading) exists between light (U62, yellow shading), and dark (U76, top row) genes tested in transgenic assays. This change is a mutation derived in the U62 line, with respect to outgroups, and the majority consensus of all melanogaster sequences used.

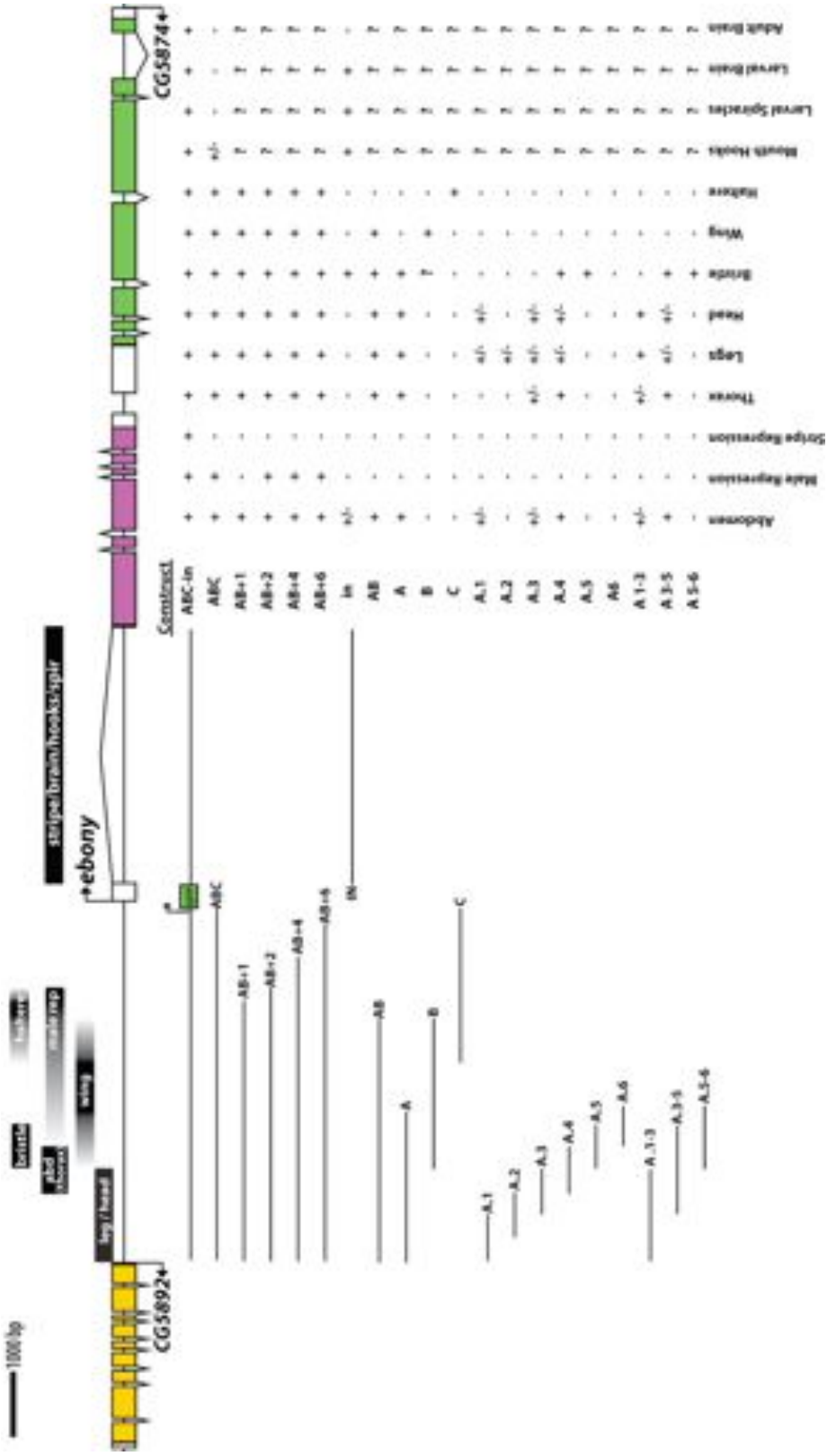
1000 bp
CG5892+
+ebony
stripe/brain/hookshair
CG5874+
Construct
ABC-in
ABC
AB+1
AB+2
AB+4
AB+6
in
AB
A
B
C
A.1
A.2
A.3
A.4
A.5
A6
A.1-3
A.3-5
A.5-6
Abdomen
Male Expression
Stripe Expression
Thorax
Legs
Head
Brain
Wing
Rubber
Mouth Hooks
Larval Spiracles
Larval Brain
Adult Brain

Figure S5

Figure S5. Mapping of *ebony* enhancers. Each bar above the locus shows the empirically determined position of each CRE of *ebony*. Black bars designate regions required for activity, while gray shading shows areas that may contribute to CRE function. Each line below the locus denotes the position of a GFP reporter construct tested for enhancer activity. To the right of each construct, a summary of expression in various tissues examined is presented. (+)designates expression, (-) indicates the lack of expression. (+/-) is used to indicate weak/ectopic or incomplete expression. (?) Marks tissues/construct combinations that were not examined

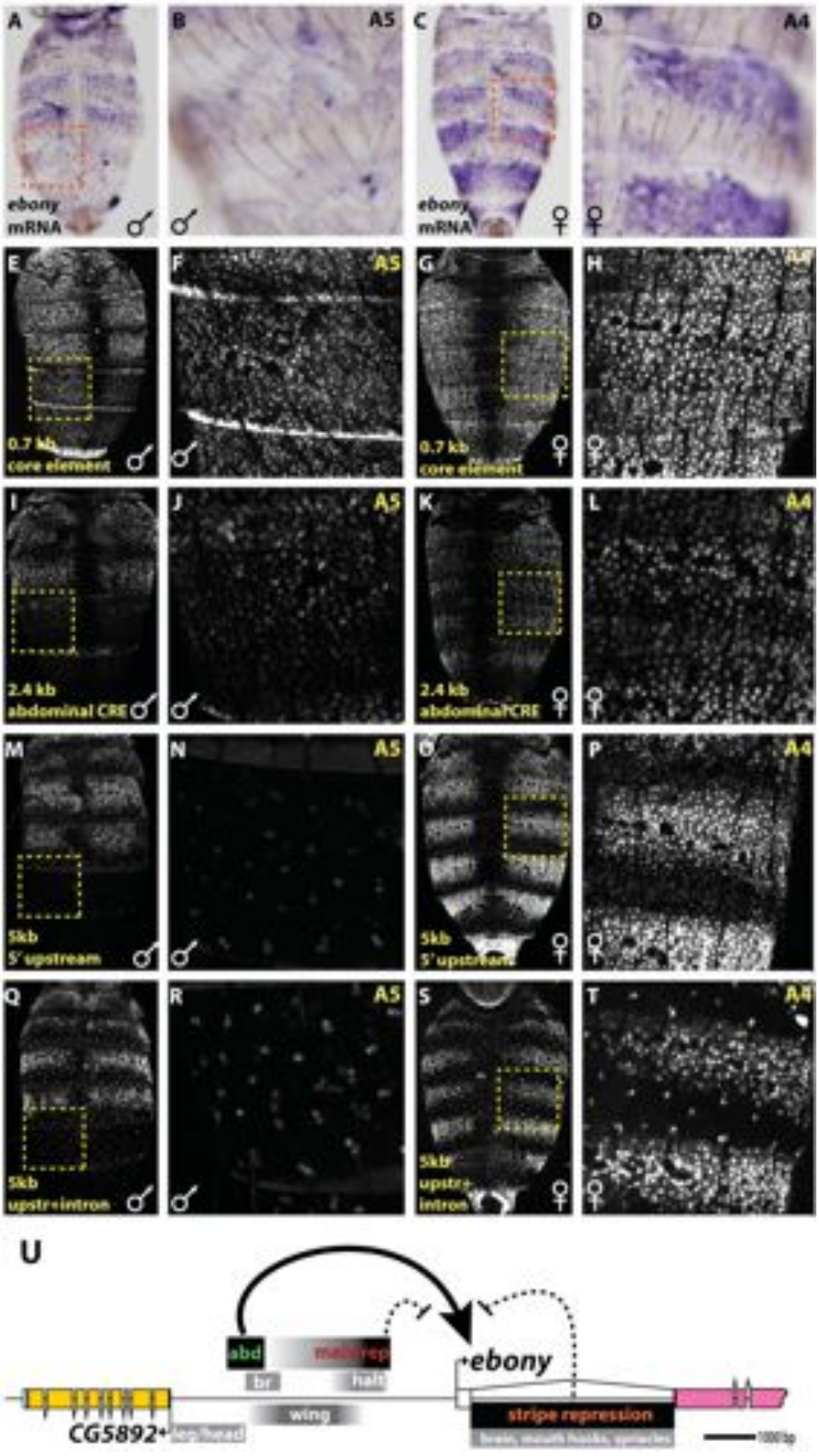
A
B
A5
C
D
A4
ebony
mRNA
ebony
mRNA
E
F
A5
G
H
A4
0.7 kb
core element
0.7 kb
core element
I
J
A5
K
L
A4
2.4 kb
abdominal CRE
2.4 kb
abdominal CRE
M
N
A5
O
P
A4
5kb
5' upstream
5kb
5' upstream
Q
R
A5
S
T
A4
5kb
upstr+intron
5kb
upstr+
intron
U
abd
br
hair
+ebony
wing
stripe repression
CG5892+

Figure S6

Figure S6. An upstream activation element is restricted by two repressive elements to generate the complete abdominal *ebony* expression pattern. (A-D) Visualization of *ebony* transcripts in the post-eclosion adult abdomen by *in situ* hybridization. (A) In males, expression is restricted from the two posterior segments, A5 and A6. Boxed region shows A5 hemitergite presented in (B). (A,C) In both males, and females, *ebony* transcript is not expressed at the posterior edge of each tergite. The Boxed region in C shows the area highlighted in D. (E-G) Promoter fusion of the 0.7 kb core element to green fluorescent protein drives expression in both the male posterior (E,F), and the posterior edge of each tergite (G,H). (I-L) Reporter activity of the 2.4 kb abdominal CRE fragment fused to GFP in male (I,J) and female (K,L) abdomens. Similar to the 0.7 kb core element, the 2.4 kb reporter drives ectopic activity in the male A5 segment (J), and at the posterior edge of each abdominal tergite (L). (M-P) By extending the reporter to the whole 5' regulatory region, expression is properly excluded from the male A5 and A6 segments (M,N), but still drives ectopic expression at the posterior edge of each tergite (P). (Q-T) Including the intron to the 3' of GFP in the context of the full 5' regulatory fusion construct results in a precise recapitulation of the endogenous *ebony* expression pattern, with expression excluded from the posterior edge of each tergite (T). (U) Model depicting the action of the three separate modules (one abdominal activation element, a male repression element, and a stripe repression element) in spatially restricting *ebony* expression in the abdomen.

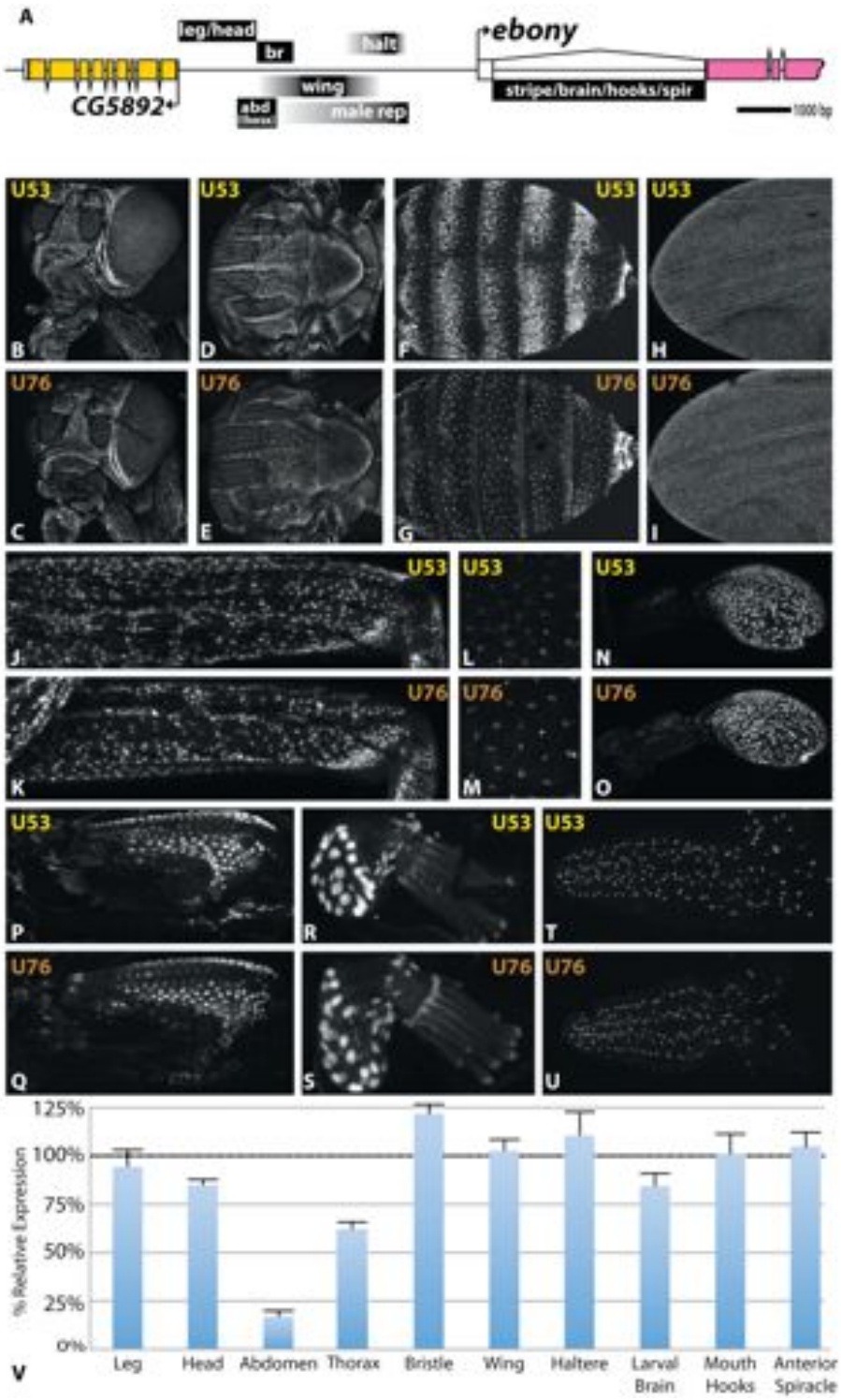
A
leg/head
br
halt
ebony
wing
CG5892
abd
male rep
stripe/brain/hooks/spir
1000 bp
U53
U76
B
C
D
E
F
G
H
I
J
K
L
M
N
O
P
Q
R
S
T
U
V
% Relative Expression
125%
100%
75%
50%
25%
0%
Leg
Head
Abdomen
Thorax
Bristle
Wing
Haltere
Larval Brain
Mouth Hooks
Anterior Spiracle

Figure S7

Figure S7. Demonstration of the modularly restricted effect of regulatory mutations. Measurement of transcriptional activity driven by modules identified in the *ebony* upstream region. (A) Map of ebony locus displaying the location of CREs mapped through reporter assays. Black bars denote regions required for activity, while gray areas delineate the area in which enhancer boundaries lie. abd, abdomen, br, bristles; male rep, male repression; halt, haltere; stripe, abdominal tergite stripe repression; brain, 3rd instar larval brain; hooks, larval mouth hooks; spir, larval spiracles. Reporter activity driven by the complete regulatory region of the *ebony* locus from a light (U53:B,D,F,H,J,L,N,P,R,S) or dark (U76:C,E,G,I,K,M,O,Q,S,U) chromosome extraction line. (B,C) Head; (D,E) Thorax; (F,G) Adult Abdomen; (H,I) Wing; (J,K) Femur of T2 Legs; (L,M) Bristles of male A6 segment; (N,O) Haltere; (P,Q) Mouth hooks; (R,S) Anterior spiracle; (T,U) third larval instar brain. (V) Quantification of relative fluorescence expressed as the percent of the light line activity. Abdominal and thoracic specificities occupy an identical stretch of regulatory DNA, and are therefore are inferred to represent the same CRE.

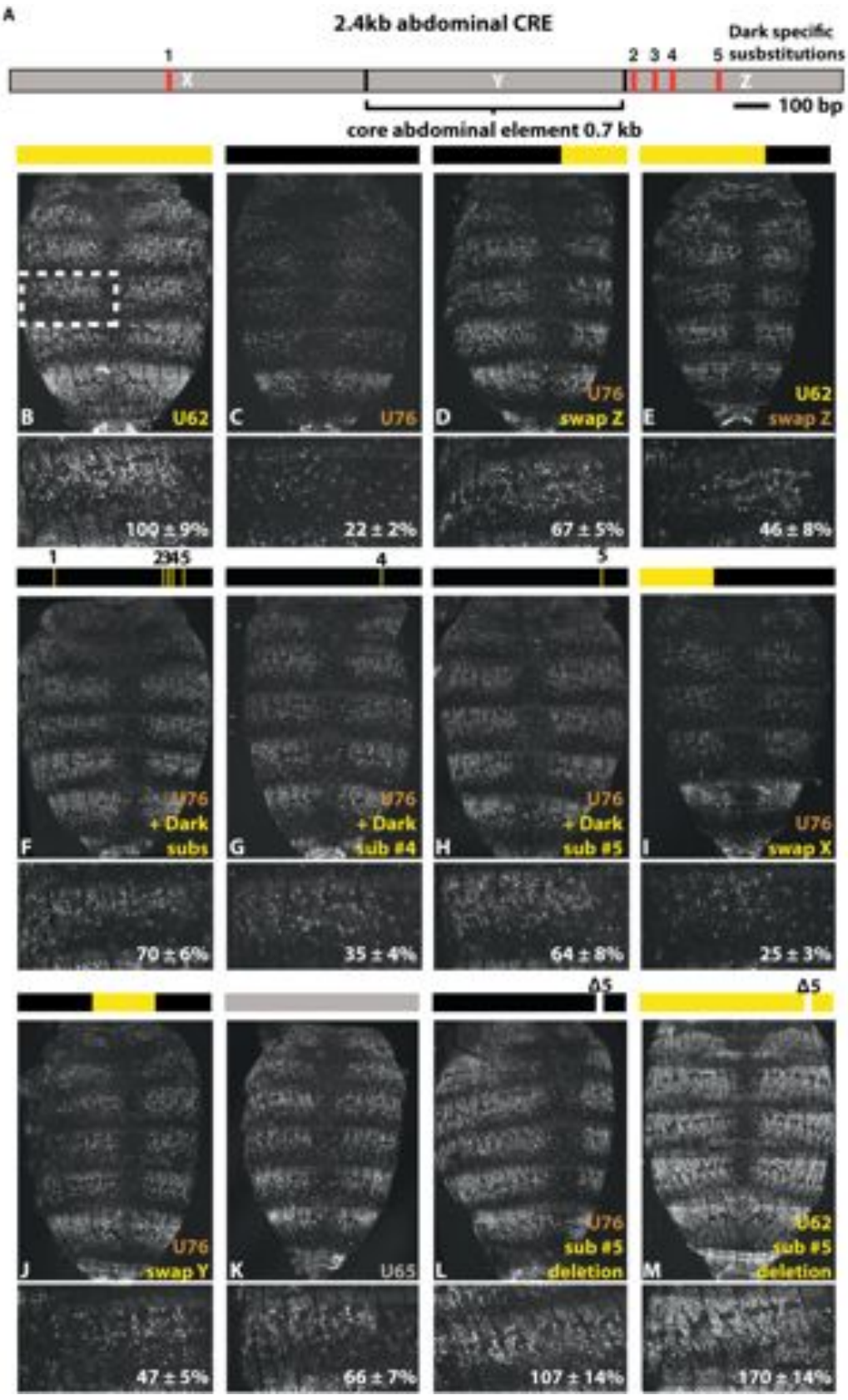
A
2.4kb abdominal CRE
Dark specific
5 susbstitutions
1
2 3 4
5
X
Y
Z
100 bp
core abdominal element 0.7 kb
B U62
C U76
D U76 swap Z
E U62 swap Z
100 ± 9%
22 ± 2%
67 ± 5%
46 ± 8%
1
2345
4
5
F U76 + Dark subs
G U76 + Dark sub #4
H U76 + Dark sub #5
I U76 swap X
70 ± 6%
35 ± 4%
64 ± 8%
25 ± 3%
Δ5
Δ5
J U76 swap Y
K U65
L U76 sub #5 deletion
M U62 sub #5 deletion
47 ± 5%
66 ± 7%
107 ± 14%
170 ± 14%

Figure S8

Figure S8 Identification of subregions containing functionally relevant mutations to the *ebony* abdominal CRE. (A) Schematic of 2.4 kb reporter construct containing the *ebony* abdominal CRE. Dark specific substitutions (red bars labeled 1-5) are mutations found only in the dark haplotype block. X,Y, and Z mark fragments used to make chimeras between light and dark alleles. The boundaries of the Y fragment perfectly align to the core abdominal CRE. (B) Expression of the 2.4 kb region derived from the light line (U62). The intensity for this construct was set to 100%. (C) The dark line (U76) drives much weaker reporter expression of this identical fragment. (D) Chimeric construct where the sequence downstream of the core abdominal element ("Z" fragment) has been replaced by light allele sequence shows increased activity. (E) Construct containing the dark haplotype Z fragment in the context of the light allele 2.4 kb reporter shows decreased activity. (F) Dark strain 2.4 kb reporter in which the 5 dark specific substitutions have been reverted to the state observed for the light line has increased activity. (G) Dark strain reporter in which dark specific substitution #4 has been reverted to the light line state shows a modest increase in expression. (H) Dark allele construct in which substitution #5 has been reverted to the light line state shows a dramatic activity increase. (I) Dark strain allele construct in which the X fragment has been replaced by that of a light line confers no difference in reporter activity. (J) Chimeric construct in which the dark line's core abdominal element ("Y" fragment) has been replaced by the light line minimal element increases reporter activity of the dark allele construct. (K) Expression of the 2.4 kb reporter from the light line U65 shows intermediate expression levels. (L) Dark allele construct in which substitution #5, has been deleted, along with 5 bp on each side, has drastically increased activity, demonstrating that this sequence is required in the dark strain to decrease expression. (M) Introduction of the same 11 bp deletion into the light allele construct results in increased activity, demonstrating a role for this region in the light allele.

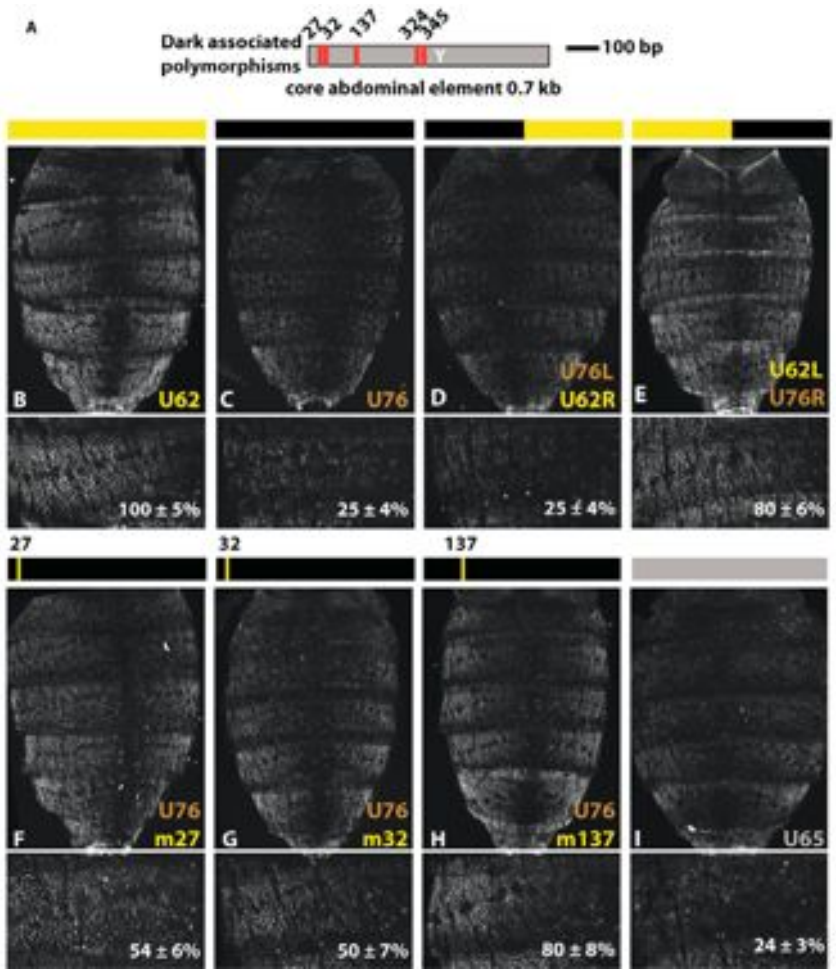

Figure S9. Pinpointing functional substitutions in the core abdominal element (Y Fragment). (A) Schematic of the Y fragment (core abdominal element). Numbered, red bars mark candidate substitutions associated with the dark haplotype block in the 5' half of the element ("Dark associated polymorphisms). (B) Abdominal activity of Y fragment derived from a light strain (U62). Expression of this construct was set to 100%. (C) The Y fragment derived from a dark allele (U76) drives weaker expression. (D) Chimeric Y fragment in which the 5' half is derived from the dark allele drives weak expression indistinguishable from that of the dark allele. (E) The reciprocal construct, containing the light allele 5' half restores expression to 80% of light allele levels. (F-H) Three constructs that individually revert candidate dark associated polymorphisms at positions 27(F), 32(G), and 137(H) show contributions to Y fragment activity. The sum of effects in F, G, and H add up to more than 100%, indicating that these mutational effects are not strictly additive. (I) The U65 core element, which is identical to the dark haplotype in the 5' half, drives similar reporter activity as the dark allele construct.

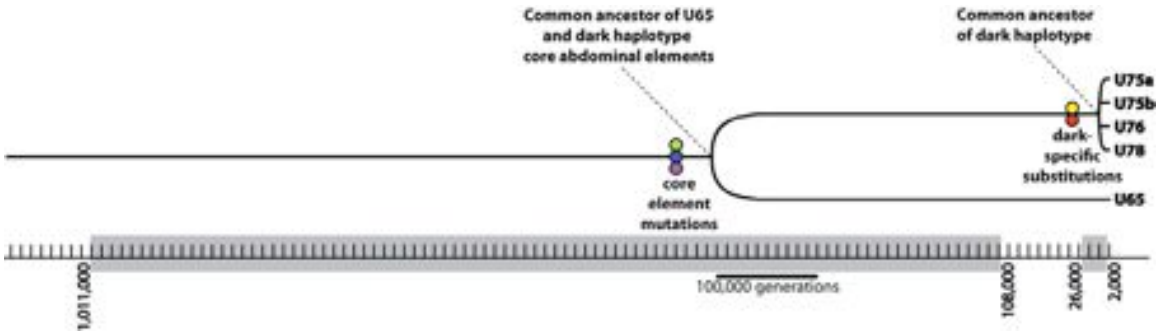

Figure S10. Estimation of haplotype divergence times. Tree depicting the evolutionary history of the abdominal CRE, showing how the core element of U65 shared a common ancestor with the dark alleles, before the latter hitchhiked to high frequency. Divergence time estimations indicate that the core element of U65 and the dark haplotypes diverged between ~108,000 and 1,011,000 generations ago, while the dark haplotype did not reach high frequency until 2,000 – 26,000 generations ago.

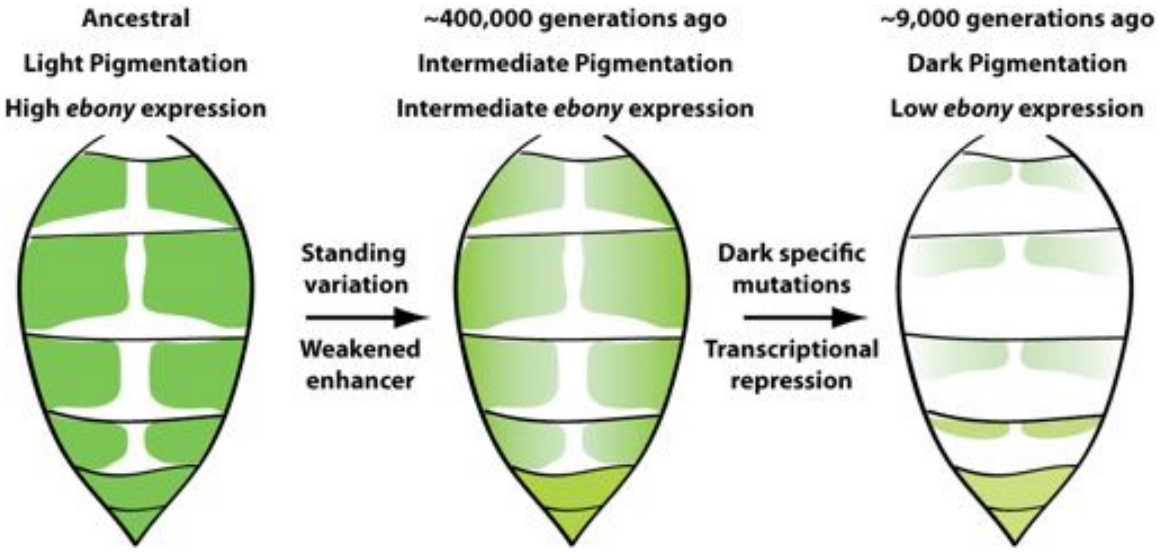

Figure S11. The genetic path of morphological evolution at a modular *cis*-regulatory element enhancer. Schematic depicting the stepwise evolution of the abdominal enhancer CRE, *ebony* mRNA expression, and the adult pigmentation phenotype. The five functional substitutions arose from both standing variation and new mutations and combined to produce a large gene effect. Green shading represents *ebony* expression level.

Table S1. Quantification of ebony mRNA expression in Ugandan chromosomal extraction lines.

Strain	Signal	%Max	% SEM
U53 (#18)	53.86	88.00%	7.28%
U62 (#54)	61.21	100.01%	9.90%
U64 (#1)	31.00	50.65%	9.42%
U65 (#29)	30.67	50.10%	7.91%
U75 (#45)	10.50	17.15%	4.71%
U75 (#50)	12.10	19.77%	5.67%
U76 (#40)	14.58	23.83%	4.20%
U78 (#17)	25.92	42.34%	4.51%

Table S2. Quantification of reporter construct activities

2.4 kb abdominal CRE reporters

Construct	N	Relative activtiy	SEM	Effect (vs U76)
U76	38	22.1%	2.0%	
U78	14	21.7%	3.6%	
U65	17	63.1%	5.1%	
U53	15	97.7%	6.2%	
U62	18	100.0%	8.8%	
U76swapX	8	23.1%	3.1%	
U76swapY	22	46.6%	5.3%	
U76swapZ	23	66.9%	5.2%	
U76 + dark specific subs	14	70.2%	5.9%	
U62swapY	16	99.1%	8.4%	
U62swapZ	7	46.0%	8.0%	
U76 dark sub #2 reversion	6	24.8%	5.6%	
U76 dark sub #3 reversion	12	27.3%	5.2%	
U76 dark sub #4 reversion	12	35.3%	3.8%	**13.1%**
U76 dark sub #5 reversion	14	63.9%	7.7%	**41.7%**
U76 dark sub #5 deletion	12	105.8%	11.3%	
U76 dark sub 2-5 deletion	9	91.4%	12.4%	
U76 dark sub 2-3 deletion	12	21.4%	4.8%	
U62 dark sub #5 deletion	16	169.9%	13.9%	
U62 dark sub 2-5 deletion	5	127.5%	24.2%	
U62 dark sub 2-3 deletion	9	151.0%	20.0%	

0.7 kb core abdominal element reporters

Construct	N	Relative activtiy	SEM	Effect normalized to 2.4 kb construct (vs U76)
U76	13	24.6%	4.2%	
U65	18	24.3%	3.1%	
U53	9	89.4%	6.9%	
U62	21	100.0%	5.3%	
U76 m27	15	54.4%	6.2%	**9.7%**
U76 m32	7	50.3%	7.3%	**8.3%**
U76 m137	4	79.9%	7.8%	**18.0%**
U76 m324	3	17.8%	7.7%	
U76 m345	4	26.6%	4.9%	
U76L U62R	10	24.5%	3.5%	
U62L U76R	10	81.0%	6.0%	
U62L U65R	4	102.6%	12.8%	
Canton S	8	151.2%	12.8%	

Table S3. Primers used to create GFP reporter constructs.

Construct	Forward Primer	Reverse Primer	Restriction Sites
ABC-in (upstream)	TTCCGggcgcgccTAAGCGATGTCTGGTGCTGGTCTG	TTGCCcctgcaggATTCGGCTGGCGAAGAATGACTGA	*Asc I/ Sbf I*
ABC-in (downstream)	tatcttaactagtcaAACTCGCTTTCCCGAAATTAATGTGC	tatcttaactagtcaTTGGGCTTAGAATCTCAGTCGGAGAA	*Spe I/ Spe I*
ABC	TTCCGggcgcgccTAAGCGATGTCTGGTGCTGGTCTG	TTGCCcctgcaggATTCGGCTGGCGAAGAATGACTGA	*Asc I/ Sbf I*
AB+1	TTCCGggcgcgccTAAGCGATGTCTGGTGCTGGTCTG	TTGCCcctgcaggATCTGTGTAATAGTCAGGAGATTT	*Asc I/ Sbf I*
AB+2	TTCCGggcgcgccTAAGCGATGTCTGGTGCTGGTCTG	TTGCCcctgcaggTGAGTGTTTCGTACAAGAATCAAC	*Asc I/ Sbf I*
AB+4	TTCCGggcgcgccTAAGCGATGTCTGGTGCTGGTCTG	TTGCCcctgcaggGTAGTAGGTTGTTAGTACTCGTGC	*Asc I/ Sbf I*
AB+6	TTCCGggcgcgccTAAGCGATGTCTGGTGCTGGTCTG	TTGCCcctgcaggCTAATTGGCAGGCGAATTGTACAC	*Asc I/ Sbf I*
in	TTCCGggcgcgccCCCACGGTACGTATTACGTGAT	TTGCCcctgcaggTGGCAGCGAACCCATCTTGAAG	*Asc I/ Sbf I*
AB	TTCCGggcgcgccTAAGCGATGTCTGGTGCTGGTCTG	TTGCCcctgcaggTAAGCGACTGAAAGGCGTGCTGAGCA	*Asc I/ Sbf I*
A	TTCCGggcgcgccTAAGCGATGTCTGGTGCTGGTCTG	TTGCCcctgcaggTCTGGAAGTGTGGAGCACCTCCAT	*Asc I/ Sbf I*
B	TTCCGggcgcgccGGTCTTGTTTGTCCGTATGAGCATCC	TTGCCcctgcaggTAAGCGACTGAAAGGCGTGCTGAGCA	*Asc I/ Sbf I*
C	TTCCGggcgcgccCGGTTCGCCTTTCATAATATGTCG	TTGCCcctgcaggATTCGGCTGGCGAAGAATGACTGA	*Asc I/ Sbf I*
A.1	TTCCGggcgcgccTAAGCGATGTCTGGTGCTGGTCTG	TTGCCcctgcaggGAAAGAAATAGTTTGGGGCACCTG	*Asc I/ Sbf I*
A.2	TTCCGggcgcgccGCCGGTAATTTAAACACGCGTGTG	TTGCCcctgcaggAGCACCTGAGAACCGATTCGAACG	*Asc I/ Sbf I*
A.3	TTCCGggcgcgccCAGGTGCCCCAAACTATTTCTTTC	TTGCCcctgcaggGGATGCTCATACGGACAAACAAGACC	*Asc I/ Sbf I*
A.4	TTCCGggcgcgccCGTTCGAATCGGTTCTCAGGTGCT	TTGCCcctgcaggCATAGAACTTGCAAAGCTTAGTAC	*Asc I/ Sbf I*
A.5	TTCCGggcgcgccGGTCTTGTTTGTCCGTATGAGCATCC	TTGCCcctgcaggTAATCAAGTTTCTTTATGAGCTAG	*Asc I/ Sbf I*
A.6	TTCCGggcgcgccGTACTAAGCTTTGCAAGTTCTATG	TTGCCcctgcaggATAACCATCTTAATCGCAAACGTG	*Asc I/ Sbf I*
A 1-3	TTCCGggcgcgccTAAGCGATGTCTGGTGCTGGTCTG	TTGCCcctgcaggGGATGCTCATACGGACAAACAAGACC	*Asc I/ Sbf I*
A 3-5	TTCCGggcgcgccCAGGTGCCCCAAACTATTTCTTTC	TTGCCcctgcaggTAATCAAGTTTCTTTATGAGCTAG	*Asc I/ Sbf I*
A 5-6	TTCCGggcgcgccGGTCTTGTTTGTCCGTATGAGCATCC	TTGCCcctgcaggTCTGGAAGTGTGGAGCACCTCCAT	*Asc I/ Sbf I*

Table S3 (Continued)

Primers for Ugandan allele constructs

Constructs	Forward Primer	Reverse Primer	Restriction Sites
Full regulatory complement (5', upstream of GFP)	TTCCGggcgcgccTTCACTCACTCTCCCACTGACTCCCA	TTGCCcctgcaggCCTGCTCTTAMAGCCSCTGCAATTAC	*Asc I/ Sbf I*
Full regulatory complement (intron, downstream of GFP)	tatcttaactagtcaAACTCGCTTTCCCGAAATTAATGTGC	tatcttaactagtcaTTGGGCTTAGAATCTCAGTCGGAGAA	*Spe I/Spe I*
2.4 kb abdominal CRE	TTCCGggcgcgccTAAGCGATGTCTGGTGCTGGTCTG	TTGCCcctgcaggATAACCATCTTAATCGCAAACGTG	*Asc I/ Sbf I*
core element	TTCCGggcgcgccTCTGGTAATTCAAAAACGCCTG	TTGCCcctgcaggGATTAGTATCCGTTAGAAACATAG	*Asc I/ Sbf I*

Table S4. Primers used to create mutant GFP reporter constructs.

Primer name	Primer	Notes
ebA1-3swap-R	CAGGCGTTTTTGAATTACCAGA	Reverse primer used to amplify X fragment for overlap extension
ebA4swap-F	TCTGGTAATTCAAAAACGCCTG	Forward primer used to amplify Y fragment for overlap extension
ebA4swap-R	GATTAGTATCCGTTAGAAACATAG	Reverse primer used to amplify Y fragment for overlap extension
ebA5-6swap-f	CTATGTTTCTAACGGATACTAATC	Forward primer used to amplify Z fragment for overlap extension
4Emid-F	ATT TCA GTT CCT ATA AAG TAT A	Forward primer used to make right-hand side of core element chimeras
4Emid-R	TAT ACT TTA TAG GAA CTG AAA T	Reverse primer used to make left-hand side of core element chimeras
Dark Specific 1 F	CGTAAAGTTGATTgCGATTATATGTAGG	Primer (Forward) used to mutate Dark specific mutation #1
Dark Specific 1 R	CCTACATATAATCGcAATCAACTTTACG	Primer (Reverse) used to mutate Dark specific mutation #1
Dark Specific 2 F	TAATCTTATTGCCcATTCAATCTAAACA	Primer (Forward) used to mutate Dark specific mutation #2
Dark Specific 2 R	TGTTTAGATTGAATgGGCAATAAGATTA	Primer (Reverse) used to mutate Dark specific mutation #2
Dark Specific 3 F	TTGAGAAAGTACTaTCAATATACAAGGA	Primer (Forward) used to mutate Dark specific mutation #3
Dark Specific 3 R	TCCTTGTATATTGAtAGTACTTTCTCAA	Primer (Reverse) used to mutate Dark specific mutation #3
Dark Specific 4 F	ATCCTCTAATAAAACTGAATACCTAAA	Primer (Forward) used to mutate Dark specific mutation #4
Dark Specific 4 R	TTTAGGTATTCAGTTTTATTAGAGGAT	Primer (Reverse) used to mutate Dark specific mutation #4
Dark Specific 5 F	TTGCTGGGCTTTAAaGTTTTCAGGTGT	Primer (Forward) used to mutate Dark specific mutation #5
Dark Specific 5 R	ACACCTGAAAACtTTAAAGCCCAGCAA	Primer (Reverse) used to mutate Dark specific mutation #5
Core mut 27	TTCCGggcgcgccTCTGGTAATTCAAAAACGCCTGTGCCc GTTCAAATCGGTT	Modified forward primer forward primer for core construct. Primer contains an *Asc I* site (lowercase)
Core mut 32	TTCCGggcgcgccTCTGGTAATTCAAAAACGCCTGTGCCT GTTCgAATCGGTTCTCAG	Modified forward primer forward primer for core construct. Primer contains an *Asc I* site (lowercase)

Core mut 137 F	GATCTTTTCAATTAGTAAATTAACATAAGTCTGGT	Primer (Forward) used to make core mutation at position 137
Core mut 137 R	ACCAGACTTATGTTAATTTACTAATTGAAAAGATC	Primer (Reverse) used to make core mutation at position 137
Dark specific 5 Deletion F	AAATATTGCTGGGCTCAGGTGTTTTCTAG	Primer (Forward) used to delete Dark specific mutation #5 +10 bp
Dark specific 5 Deletion R	CTAGAAAACACCTGAGCCCAGCAATATTT	Primer (Reverse) used to delete Dark specific mutation #5 +10 bp